Numerical simulations to understand spatial sedimentation characteristics in a shallow reservoir

SUBHASRI DUTTA[1], Harshvardhan Harshvardhan[2], and Dhrubajyoti Sen[1]

[1]Indian Institute of Technology Kharagpur
[2]Indian Institute of Technology Delhi

April 28, 2020

Abstract

Sedimentation is a great concern for designers and managers of reservoirs, as it is responsible for reduction of reservoir's operational life. This inevitable but unfortunate phenomenon reduces storage capacity of reservoirs and diminishes utility of infrastructure. Therefore, a hitherto unexplored and unreported area of sedimentation in reservoirs – spatial distribution of deposited sediment in a shallow reservoir – is investigated, employing numerical simulation model (TELEMAC-SISYPHE). Present study considers the Hirakud Dam on the River Mahanadi in eastern India as a test case. The study established generic trends between reservoir geometry variables and sediment distribution patterns in a reservoir through a heuristic set of numerical experiments for several configurations of reservoirs. The research work comprises of the following steps: Defining significant geometric parameters defining any typical water storage reservoir; Setting up and running numerical model for simulating flow and sediment movement for a range of possible geometries; Expressing characteristic parameters defining extent of sedimentation (height of sediment mound, spatial width, longitudinal extent) in terms of reservoir geometric parameters; Validating proposed generic relations with field observations of sedimentation of the Hirakud Reservoir within its two branches of Mahanadi and Ib. The study shows that the reservoir geometry and bathymetry significantly influence the flow velocity which, in turn, dictates the conditions of sediment transport and deposition within the reservoir. Lateral spread of sediment increases with an increase of expansion angle resulting in lower peaks of sediment dunes. Increase in cross slope increases the flow velocity, causing higher movement of sediments. Further, cross slope has direct influence in increasing transverse movement of sediment towards central dip resulting in a narrower sediment footprint across the reservoir section. Maximum height of evolution moves upstream, while minimum isoline moves downstream with an increase of longitudinal slope. The developed relations would be helpful to the reservoir managers in understanding the nature of bed elevation rise in respective reservoirs and for arranging proper desiltation of sediments for conserving reservoir capacity.

1 INTRODUCTION

Human activity, like construction of dams and reservoirs, alter the dynamic balance of water flow and sediment budget. On entering a reservoir, the flow velocity, turbulence, bed shear stress and transport capacity of a river decrease, resulting in deposition of sediment particles to form a delta in the headwater zone, ultimately extending further into the reservoir with the passage of time. This progressive deposition of sediments has a negative impact on the flood mitigation performance of a reservoir and reduces its storage capacity.

Various studies (Garde et al., 1990; Ranga Raju et al, 1999) were carried out to develop the empirical and semi-empirical methods to determine the amount of sediment deposits. Stovin (1996) studied the influence of several physical parameters on the flow rate, reservoir geometry etc. The bed shear stress distribution was found to play an important role on the sediment deposits. Morris and Fan (1998) analysed in details the deposition patterns in various types of reservoirs. They concluded that the sediment deposition patterns along the longitudinal direction vary significantly from one reservoir to another depending on their geometry, discharge, sediment characteristics, reservoir operation, etc. Most of the sediments are transported within the reservoirs up to the point of deposition by the following three processes: 1) transport of coarse particles as bed load along the reservoir surface, 2) transport of fine particles by turbidity density currents and 3) transport of very fine particles as non-stratified flow. Initially, the longitudinal growth of the deposition remains rapid due to the shallow and low storage capacity of the upstream reservoir. Rahmanian and Banihashemi (2011) proposed a new semi-empirical technique based on the reservoir geometry characteristics for evaluating cumulative sediment distribution along the reservoirs in the longitudinal direction. Further, Behrangi et al. (2014) predicted the sediment amount and longitudinal distribution pattern for estimation of the useful lifespan of reservoirs and identification of optimal locations for intakes and outlets at the initial stages of dam design.

The characteristics of complex flow pattern in rectangular shallow reservoirs have also been discussed thoroughly (Kantoush and Schliess, 2009; Camnasio et al., 2011 and Peltier et al., 2015). These studies mainly focused on the experimental investigations pertaining to flow characteristics in shallow rectangular reservoirs. Different flow fields were observed either with no reattachment of flow or a jet with one or multiple reattachment points depending on the size of the reservoir. Kantoush (2008) showed that reduction of length of a rectangular shallow reservoir induced a transition from an asymmetrical flow with one reattachment point to a symmetrical flow without any reattachment point. Also, different numerical simulations were conducted to analyse the sediment transport capacity (Lu and Wang, 2009; Zhou et al., 2009), settling velocity (Zhou et al., 2009) and sedimentation quantity (Gao et al., 2015).

The determination of hydraulic properties is a pre-requisite for sediment transport modelling in general. The modelling approach enables the calculation of reservoir life expectancy, the trapping efficiency of the reservoir, the amount of the released sediments downstream of the reservoir and the simulation of several reservoir sediment management scenarios.

Sediment transport is important in case of affecting water quality and the life expectancies of the reservoirs. Therefore, it is one of the most important factors that should be considered and well assessed in design of reservoirs. Studies about sediment transport mainly focused on hydrodynamic processes and their driving forces to understand how sediments are eroded, transported, deposited, and re-suspended in different water systems through numerical modelling and surveying of reservoirs (Blumberg and Mellor, 1987; Mehta et al., 1989).

Empirical formulae based on laboratory data are not always accurate enough and unable to replicate the true field conditions properly due to the error in the scale ratio and fluid properties. Also, field data based on empirical formulae suffer from subjective errors. To overcome these difficulties, computational fluid dynamic tools may be used to predict hydrodynamic and morphodynamic parameters within the reservoir subjected to varying flow conditions.

White (2001) summarised that 1-D model is suitable for long-term simulation of reservoir sedimentation with elongated channel geometry, while 2-D or 3-D models require much more field data for calibration. 1-D computational models provide information in a section-averaged manner without giving any information about the flow characteristics in the vertical and transverse directions. A 1-D model usually solves differential conservation equations of mass and momentum for the water, along with sediment transport mass continuity equations using finite difference methods (Papanicolaou et al., 2008). Normally, the models employ rectilinear coordinate system; however, some of them also use curvilinear systems. Some of the widely used one dimensional models for simulation of sediment behaviour in rivers and reservoirs are HEC-6 (USACE, 1993), FLUVIAL-12 (Chang, 1998), CONCEPTS (Langendoen, 2000), CCHE1-D (Wu and Vieira, 2002), MIKE11 (DHI, 2003), etc. for erosion, sediment transport and deposition in straight channels and rivers.

The depth-averaged 2-D models divide the total computational domain into a network of two-dimensional elements. However, no variation is considered in the vertical direction. Two dimensional models are most popular than others as they provide enough information of the computed parameters in the project assessment. The 2-D models solve the depth-averaged form of the Navier-Stokes equations, with sediment transport models having capabilities to describe both bed and suspended load. These models assume the velocity of water and the concentration of sediment to be uniform through the water column. So, these models do not take into account secondary flow effects. Some of the widely used two dimensional sediment transport models include TABS-MD (Thomas and McAnally, 1990), HSCTM2-D (Hayter, 1995), CCHE2-D (Wu, 2001) MIKE21 (DHI, 2003), and SRH-2-D (Lai et al., 2008).

3-D numerical models are based on the assumption of hydrostatic pressure distribution in vertical direction and provide information in all the three directions within the reservoir. The 3-D models are avoided unless very detailed distribution of different parameters needs to be simulated in accounting with flow characteristics in all directions. Although they are the most complicated and resource consuming in implementation, they are nevertheless the most informative as they include all the space dimensions. The 3-D models solve the Navier-Stokes equation using numerical approaches such as the finite element, finite difference or finite volume method (Papanicolaou et al., 2008). Some of the most widely used three dimensional models are SSIIM (Olsen, 1994), Delft-3-D (WL | Delft Hydraulics, 2006), ECOMSED (HydroQual, 2002), CCHE3-D (Stone et al., 2007).

In recent years, several 2-D and 3-D numerical morphodynamic models have been developed that have the capability to predict bed deformation in channels with non-moving boundaries. Minh Duc et al. (2004) proposed a 2-D depth-averaged model using a finite volume method with boundary-fitted grids and fixed channel sides. Wu and Wang (2004) proposed a 2-D depth-averaged model for computing flow and sediment transport in curved channels, simulating sediment transport in a channel bend with fixed sides. A 3-D model for the calculation of flow and sediment transport was proposed by Wu et al. (2000). Suspended load transport was simulated through the general convection-diffusion equation with an empirical settling velocity term. Bed load transport was simulated with a non-equilibrium method and the bed deformation was obtained from an overall mass-balance equation. Elci et al. (2007) discussed the erosion and deposition of cohesive sediments in a thermally stratified reservoir using a 3-D numerical model for different conditions. They reported that though sedimentation in a reservoir is often modelled considering only the deposition of sediments delivered by tributaries, the sediments eroding from the shorelines could have significant effects to the sedimentation in the reservoir. Choi and Lee (2015) numerically predicted the total sediment load in a river, using information on channel geometry and slope, discharge and the size of bed materials. They also carried out the flow analysis using the lateral distribution method, which distributes the flow and sediment load across the width, based on channel geometry and flow dynamics. Faghihirad et al. (2015) applied numerical model to Hamidieh Reservoir in Iran, associated with a dam, water intakes and sluice gates, in order to investigate the flow patterns and sediment transport processes in the vicinity of the dam. They found that an excess of sedimentation in a reservoir leads to sediment entrainment in waterway systems and hydraulic schemes.

However, these studies have been done to find out the progress of reservoir sedimentation along the longitudinal and lateral directions, as its lateral spreading (spatial distribution) has not been investigated much. Also, there has been little effort to estimate actual siltation in a shallow reservoir using physical based numerical simulation models. Further, limited studies appear to have been carried out on the influence of different geometric parameters of a trapezoidal channel on the pattern of sedimentation. Therefore, the present study has been done to find out the progress of reservoir sedimentation along the longitudinal and lateral directions, as its lateral spreading (spatial distribution) has not been investigated much. Also, there has been little effort to estimate actual siltation in a shallow reservoir using physical based numerical simulation models. Further, limited studies appear to have been carried out on the influence of different geometric parameters of a trapezoidal channel on the pattern of sedimentation.

2 PROBLEM FORMULATION

Dutta and Sen 2016 discussed the sediment deposition characteristics in the reservoir of the Hirakud Dam, in India, which has occurred in the past and their likely impact on the reservoir performance. Though the analyses are specific to the Hirakud Reservoir, a curious observation comes to light while observing the sedimentation patterns in the reservoirs of the two Rivers, Mahanadi and Ib, that flow into the reservoir. It appears from the sequence of simulated progressive reservoir sedimentation patterns that the sediment deposition at the bottom of River Mahanadi is somewhat different than that for River Ib. While the sediment in the former basin appears to deposit along the deep channel – more towards the centre of the river valley – in the latter it appears to deposit along the edges. This distinction is not directly noticeable from the measured bathymetry maps of the reservoir which, anyway, is very scanty. The minute differences, observable in the numerical simulation results, almost certainly appear to depend on the variables causing sedimentation, like the size of the sediment particles, flow velocity and depth, apart from the geometrical characteristics of the reservoir itself. Since the sediment size and flow variables are nearly the same in the two Rivers (Mahanadi and Ib) during the passage of floods, when the maximum deposition takes place, the difference in deposition patterns is likely to be caused by the uniqueness in the geometrical properties of the two rivers. Though a large body of literature exists reporting the progress of deposited sediments in a reservoir along the longitudinal direction of river flow, not many examine the spatial distribution pattern of sediments in an artificially formed reservoir behind a dam. Therefore, the objective of this research work is to inquire into the reasons governing the reservoir sedimentation patterns and to establish any generic trend that may exist connecting the reservoir geometry variables and the sediment distribution patterns in a reservoir through a series of numerical experimentations.

Transportation and deposition of sediment are governed primarily by the flow velocity. Sediment particles transported by the flow induces morphodynamic changes on the bed. As a result, in an artificial reservoir where the flow field of a natural river gets substantially altered, the modified velocity pattern has a significant influence on the spatial pattern of the sediment deposited at the reservoir bottom. This, therefore, intuitively leads to suggest that it may be possible to identify certain characteristic geometrical parameters defining reservoirs which, when varied, can result in different patterns of sedimentation.

The velocity of flow in a reservoir, if idealised as having a trapezoidal shape in plan, is likely to reduce more if it widens over a relatively short distance. This may cause the suspended sediment being brought in by the river to get deposited close to its entry point to the reservoir. On the other hand, in a narrow reservoir, the velocity may not reduce significantly along its length and the sediment deposition on the reservoir floor may get elongated along the downstream direction. Hence, the average expansion angle of the reservoir walls in plan (α) is considered here as the first parameter by which a reservoir may be characterised. On similar reasoning, the average bed slope measured along the length of a reservoir, that is the longitudinal slope (SL), appears to be another governing parameter since with a greater slope, the rate of increase of depth would be more along the flow direction, leading to a rapid decrease in the flow velocity. Finally, the bottom profile of the reservoir bed also appears to play a role in the spatial distribution of sediments. Dutta and Sen 2016 indicated that the Ib, smaller of the two rivers contributing flow to the Hirakud Reservoir, has a relatively flat bottom as compared to that of the Mahanadi. It may be presumed that the cross slope of the reservoir bed (which is more in case of the Mahanadi branch) may help in driving the depositing sediment towards the central spine of the reservoir, resulting in a single deposition track at the bottom. Conversely, a flatter reservoir bed may not let this happen (as for the Ib branch) and the sediment is likely to spread out spatially, more like an alluvial fan. Hence, the average cross slope of the bed (SC) of a reservoir is considered here as the third important characteristic parameter influencing the deposition pattern of the sediments on the floor of the reservoir.

Although the above parameters may be estimated approximately for any reservoir created by a dam across a river, it is difficult to obtain a direct analytical relation connecting the spatial sediment deposition patterns in terms of the governing variables. For the present work, therefore, the validated TELEMAC-2D model [as demonstrated in (Dutta and Sen, 2016)] is employed in carrying out numerical experimentation by varying the three parameters (α, *SL* and *SC*) for different hypothetical reservoir geometries and analysing the features of the deposited sediments. The generic trends from these series of numerical experiments are used at the end of this paper for explaining the unique sedimentation patterns mentioned earlier for the Mahanadi and Ib River branches of the Hirakud Reservoir. The work presented in this paper attempts to fill in this gap by proposing a methodology by which any reservoir that can be approximated by the characteristic parameters α, *SL* and *SC*, the resulting spatial sediment deposition pattern on its bed can be predicted

3 MODEL SET-UP

Numerical simulations of flow characteristics along with sedimentation are performed on the hypothetical reservoirs with the common computational mesh for the numerical 2-D flow simulation model TELEMAC (Desombre, 2013) and the sediment transport model SISYPHE (Tassi, 2014). The model TELEMAC-2D solves the depth-averaged Saint-Venant equations (conservation of mass and momentum) using the finite element formulation over the computational domain. SISYPHE computes the sediment transport and predicts the evolution of the reservoir bed by solving the Exner equation. Descriptions of the models in greater details have been provided in Dutta and Sen, 2016; where these were demonstrated for simulating the morphological changes in the Hirakud Reservoir due to sedimentation. Although previous studies reported the use of the coupled hydrodynamic and sediment transport model (TELEMAC-SISYPHE) for simulating sedimentation (Villaret et al., 2013; Hostache et al., 2014), this is a first attempt to apply TELEMAC-SISYPHE numerical 2-D model to generate some relations in between the reservoir geometry and sediment distribution pattern.

An idealised reservoir geometry is modelled (Figure 1), defined by the three characteristic parameters α, *SL* and *SC*. The length of the reservoir is kept constant at 10 km. The unstructured triangular mesh was generated with the help of the graphical user interface BlueKenue (2012). The mesh size used in each of the experiments is in the order of 50 m. Figures 2(a) to 2(c) illustrate the generated triangular mesh for the entire computational area of a typical idealised reservoir geometry, along with the bottom elevations. The same domain has been replicated for different parameters, permitting the evaluation of the hydrodynamic response of idealised reservoir having different configurations.

The geometric and hydraulic conditions of the simulations are initially set up to schematize the sediment flow into the reservoir domain. Since the primary objective of this study focuses on the influence of the reservoir geometry (expansion angle, longitudinal slope and cross slope), the characteristics of flow and sediment are kept constant for all the simulations. The mean diameter of sediment is set as 30 µm and uniform sediment gradation is assumed. Non-uniform sediments are not assumed in the present study since the sedimentation characteristics of such particles is likely to vary widely over the extent of the reservoir. The inflow rate of sediment in the domain is chosen in such a way that the volumetric concentration corresponds to those observed in the field. SSC (Suspended sediment concentration) is set equilibrium to avoid unwanted erosion and deposition. The vertical variations of SSC are considered negligible in comparison to its horizontal equivalents. The reservoir depths in the experiments have been kept an order of magnitude smaller than the lateral dimensions as generally encountered in wide reservoirs, ensuring that the vertical velocity component remains negligible and the flow may reasonably be represented by the shallow water equations.

Two open boundaries for the domain are defined, one on the upstream and the other on the downstream. The width of the inlet and outlet of the domain are kept equal. Following the monsoon period of 4 months, the simulations were also continued for 4 months, which generate maximum amount of annual sediment load. A constant inflow discharge is prescribed as the upstream boundary condition for all the cases considered and a constant water depth, corresponding to normal operating water level, is specified at the downstream boundary. The rest of the points along the periphery of the closed domain are considered as a closed boundary. Figure 3 shows the inlet and outlet boundaries respectively of a typical domain.

The simulations for each case are carried out until a steady state is reached and no meandering jet is observable within the domain. The initial sediment concentration of water is assumed to be zero, that is, clear water. As discussed in some of the previous studies like Dufresne et al. (2011) and Dewals et al. (2012), a steady flow may be reached depending upon the initial condition used for running the simulation. Therefore, in all simulations, a constant value of free surface elevation is prescribed as an initial condition such that the steady state condition is achieved promptly. At each node, the water depth is calculated as the difference between the free surface elevation and bottom elevation. The frictional resistance, represented by the Strickler's roughness coefficient, is considered same for all the runs with different geometries. The constant viscosity turbulence model is considered here since it requires a lower refinement level of the mesh in comparison to the others, resulting reduced CPU time. The mass balance check is performed over the entire domain for each simulation in order to ensure physically viable result. The time step chosen, considering the optimum computation time and Courant condition, is around 4 seconds. This helps to ensure the numerical stability and convergence.

4 ANALYSIS OF RESULTS

The bed morphological process of a reservoir due to flow and sedimentation is a complex dynamic process as several factors such as development of vegetation in the river bed, presence of different hydraulic structures, etc. influence the flow velocity, which ultimately affects the morphological characteristics. Hence, this study aims at determining the morphological changes of the bed due to sedimentation in idealised trapezoidal shaped reservoir configurations. In all, 64 different configurations are run by varying the three characteristic parameters, as indicated in Table 1.

4.1 Velocity distribution

Figures 4(a) to 4(c) show the typical contours of (depth averaged) velocity and bed shear stress for simulations with various configurations. Both the velocity contours and shear stresses show similar trends across different sections for a particular configuration.

It is evident that the bed shear stress increases with increasing flow velocity resulting in an excess stress that is required to initialize the sediment motion. The flow direction is normal to the cross section of the reservoir domain and the velocity varies significantly across the channel width. The flow field remains essentially symmetric, as expected from the symmetric geometry of the models, and steady throughout all the simulations. For all the configurations, the average velocity was found to be in the range of 0.3-0.7 m/s. Initially the simulation time was set to 1 month to achieve a steady state flow condition in the reservoir. As the inlet and outlet channels are located on the opposite sides of the reservoir centreline, the flow pattern is mainly controlled by the inlet channel. The flow passes straight from the inlet to the outlet of the reservoir. Recirculation of flow [Figures 5(a) to 5(c)] is observed in the computational domain along the banks of the trapezoidal reservoir, as the outflow width is restricted symmetrically in the middle part of the downstream boundary. The width of the recirculation zones on either bank is observed to decrease with an increase in the longitudinal and cross slopes of the reservoir. The intensity of recirculation is mainly observed towards the outlet end of the domain. However, the zone increases significantly for the simulations with higher values of expansion angle due to the limited width of the outlet boundary with respect to the total downstream boundary width. As the velocity governs the mechanism of transport of sediment, the knowledge of its pattern is important to determine the spatial distribution of sediment in the reservoir.

The figures show that the maximum velocity along the centre line of the domain increases with the increase of the cross and longitudinal slope. However, the effect of expansion angle is insignificant on the magnitude of maximum velocity.

4.2 Morphological changes

Morphological variation within the computational domain is not uniform. Hence, it is interesting to visualize its evolution along the longitudinal profiles. Figures 6(a) to 6(c) show the morphological evolution of the bed within the domain. The entire domain is characterised mostly by a positive value of deposition. Only a small fraction of sediment is driven towards the outlet due to the turbulence and most of them settle down before reaching the outlet. On the other hand, erosion is visible at the entry point due to the high flow velocities generated by the narrow entrance. At the downstream, no significant change of the river bed was found due to the presence of low velocity which is not strong enough to transport the sediments towards the outlet end. Narrow peaks with decreasing heights are evident, which form closer to the inlet with the increase of the cross slope. As discussed in the previous section, the expansion angle is not found to have any effect either on the velocity distribution or on the bed evolution. This is due to the fact that the outlet and inlet widths were kept same in the simulations. Nevertheless, the maximum height of evolution of the bed marginally increases with the increase of the expansion angle. The variations are explained further in the following sections.

4.3 Maximum evolution

The following sections describe the maximum evolution of the bed within the trapezoidal reservoir:

4.3.1 Longitudinal distance of maximum evolution

Figure 7 plots the longitudinal distances (xd) at which the maximum evolution occurs against longitudinal slope for different expansion angles and cross slopes. In all simulations, because of symmetry, the maximum deposits appear along the path of the main stream of flow. The patterns of deposited sediment at various sections depend on the velocity of flow at those sections. The location of maximum values in the pattern of sediment deposits coincides with the lowest values of the velocity field. The low value of flow velocity leads to an increased value of settling velocity resulting in significantly decreasing the sediment transport capacity. Thicknesses of the deposits are represented with respect to the bed level. As evident from the graphs, xd appears to bear an inverse relationship with both longitudinal and cross slope.

4.3.2 Height of maximum evolution

Figure 8 shows the maximum height of evolutions (hd) for different configurations versus longitudinal slopes for variations of expansion angles and cross slopes. The graphs show that for the flat bottom ($SC = 0$) the velocities are significantly less to sustain sediment movement. The peak value of sediment deposition increases with the increase in longitudinal slope for flat bottom configurations only. However, velocities become significant to sustain continous sediment movement for configurations with steeper cross slope ($SC = 0.01$), that is the reservoirs with a V-shaped bottom. The dunes formed due to the deposition of sediment disintegrates due to higher velocities and consequently propelled towards the downstream of the reservoir. Thus, the peak height of the deposited mound decreases with an increase in the longitudinal and cross slope.

4.4 Minimum and maximum isolines of bed evolution

The minimum and maximum isolines within the reservoir for different longitudinal slopes and expansion angles are plotted in Figures 9(a) to 9(d). Evidently, the maximum height of evolution moves upstream of the reservoir, while the minimum isoline moves downstream towards the outlet with an increase of longitudinal slope for any given expansion angle and cross slope. This may be explained due to the phenomenon of sediments sliding along the bed, driven by gravity, since the downward component of its weight increases with an increase in the longitudinal slope. Here, too, it is visible that for any given expansion angle and longitudinal slope, the sediment gets restricted and accumulates more towards the upstream of the reservoir with the increase of the cross slope. However, the expansion angle doesn't seem to have any significant impact on the sediment deposits for higher value of cross slope. The pattern of maximum isoline is especially noticeable in case of the flat bottom reservoirs, where a horse-shoe shaped formation is observed for lower values of longitudinal slope.

Further, the isolines (value of 0.75 m) of sediment deposits at the end of 4 months are drawn for different configurations to compare the lateral and longitudinal expansion of the bed evolution (Figures 10 and 11). It is evident that for a given expansion angle, for both flat and V-shaped bottomed configurations, the 0.75 m evolution isolines move downstream towards the outlet, due to the larger sediment slides occurring at higher values of longitudinal slopes. Also, for a given longitudinal slope in a flat-bottomed reservoir, as the expansion angle increases, the 0.75 m isoline moves upstream due to increased recirculation, causing increased lateral flow of sediment. This effect is more pronounced for configurations with flat bottoms in comparison to those with V-shaped bottoms, due to an increased intensity of the flow in the central region of the reservoir.

4.5 Distribution of sediment in the transverse direction

Figure 12 shows the distribution of sediment across the transverse direction of the reservoir. The extent of transverse spread of the deposited sediment decreases and the sediment moves towards the centre of the channel due to the effect of flow with the increase of the cross slope for any given expansion angle and longitudinal slope. Here too, gravity plays an important role on attaining the threshold bed shear stress responsible for the initiation of motion of the sediment particles. For any given cross and longitudinal slope of the reservoir bottom, the transverse spread of the sediments increases with an increase in the expansion angle and shifts towards the outer edges of the reservoir.

For a reservoir with a flat bottom and having a relatively small expansion angle, there is insignificant recirculation to cause lateral spread of sediment. In contrast, for higher expansion angles, the velocities and recirculation zones significantly increase with the increase in longitudinal slope resulting in the lateral spread of sediment.

As observed from the pattern of sediment distributions, it is seen that the sediment accumulates mostly in the central region. In case of V-shaped bottom, the increase in velocities due to increase in longitudinal slope causes the sediment to move downstream rather than in the lateral direction. The rate of decrease of lateral spread of sediment distribution also changes with an increase of cross slope.

4.6 Bed morphology in the longitudinal direction

The following sections represent the change in bed morphology along the longitudinal direction for the reservoirs with flat and V-shaped bottoms.

4.6.1 Reservoirs with flat versus V-shaped bottom

The variation of the pattern of deposition with respect to the longitudinal distance for various longitudinal slopes, expansion angles and cross slopes are plotted in Figure 13. For reservoirs with V-shaped bottom cross sections, the reaches are narrow, resulting in higher flow velocities. Consequently, a significantly higher sediment transport rate is noticed in comparison to sediment deposition, whereas the opposite is observed for the flat bottomed reservoirs. Hence, it may be said that sedimentation is predominant in flat bottom reservoirs mainly during the floods due to flow with higher sediment concentration. However, sediment deposited at the bottom of V-shaped reservoirs is likely to be eroded during floods due to the higher velocity occurring along the centreline.

Figure 13 also shows that the expansion angle has no significant impact on the longitudinal sediment distribution, especially for V-shaped bottoms, with other parameters remaining constant. Some abnormality, however, is observed for flat bottomed reservoirs at very low expansion angles. This can be attributed to the fact that there is less recirculation in the transverse direction and more flow towards the centre compared to other flat bottom configurations, which causes the peak of the deposited sediment mound to move in the downstream direction.

One more observation that can be made is that for a given expansion angle of a flat bottomed reservoir, the longitudinal slope doesn't have any significant effect on the longitudinal distribution of the sedimentation pattern. The lateral flow of sediment from the sides towards the centre of the reservoir increases with the increase in cross slope. For a given cross slope, the dunes become increasingly unstable with the increase of longitudinal slope. Further, the sediment slides from the dune results in a larger foot-print in the longitudinal direction while the peak of the mound moves upstream.

4.6.2 Varying cross slope, fixed longitudinal slope and expansion angle

For a fixed value of longitudinal slope and expansion angle, the sediment gets accumulated and forms higher peak due to the reduced lateral movement with the increase in the cross slope, as shown in Figure 14. It is also observed that the dunes get steeper with an increase of cross slope. However, with the increase in sediment deposition, the cross sectional area of flow reduces, which affects the movement of the incoming sediment resulting in deposition at the bottom of the reservoir.

5 SEDIMENT DEPOSITION FEATURES IN THE HIRAKUD RESERVOIR

The generic trends from the previous sections are compared with the sedimentation features in the Hirakud Reservoir. The Rivers Mahanadi and Ib contribute the reservoirs flow and also bring in sediment from the respective catchments. However, the deposited sediment in the two river valleys exhibit different spatial distribution patterns. While the Mahanadi portion shows a single central meridional formation, that in the valley of the Ib appears to follow two branches separated some distance away from the central meridional axis. It is hypothesized that this difference is due to the variation in the physical features of the two valleys. Accordingly, measurements are taken from the river bed contours and the features, expressed in terms of the geometric variables considered in developing the generic depositional patterns, are summarized in Table 2.

From Table 2, it is evident that for the River Ib, the average values of cross slope ($SC = 0.0035$) is flatter than that of the Mahanadi ($SC = 0.007$) and at the same time, the average expansion angle ($\alpha = 20°$) is comparatively larger than Mahanadi ($\alpha = 10°$). Though the longitudinal slope for the Ib ($SL = 0.0011$) is somewhat greater than Mahanadi ($SL = 0.00073$), the first two parameters dictate the depositional pattern in this case and cause the sedimentation formation in the Ib valley to spread out and tend towards a horse-shoe shape. However, the formation in the Ib appears with two side branches of deposition and does not display a complete hose-shoe shaped geometrical pattern. This can be explained with the layout of the two rivers – Mahanadi and Ib – which shows that a flow component of the former strikes the latter within the reservoir, causing the front bar of the horse-shoe deposition to become dispersed leaving the two side branches intact along the walls of the Ib valley. Thus the deposition pattern in the Ib valley is a degenerated horse-shoe formation.

The above hypothesis is also checked with the graphs developed in this section as shown in Figures 15 to 16, respectively for the Rivers Mahanadi and Ib. The three graphs used in each case relate the height of sedimentation around (hd, expressed in m), longitudinal distance along the reservoir (xd, expressed in m) and lateral spread to the expansion angle (α), longitudinal slope (SL) and cross slope (SC). Though hd and xd are approximately the same in either case, the lateral spread is much larger for the Ib than for Mahanadi confirming the horse-shoe nature of the sedimentation in the Ib valley. The same is also confirmed by the plots of the isolines in Figure 17 respectively for the two rivers.

6 CONCLUDING REMARKS

Prediction of sediment deposition and erosion as a function of reservoir geometry, a question that has apparently not been addressed so far, is explored in this work as it is intuitively understood that the shape of a reservoir controls the velocity distribution, which in turn, affects the sedimentation process. The study made use of a numerical flow and sediment transport simulation model in analysing the deposition patterns in idealised reservoir configurations. Rather than considering a complex geometry, this study proposes representing a prototype reservoir by a few simple but quantifiable geometric parameters and assuming a regular and symmetric flow. The results of the numerical experiments, conducted on a series of 64 geometric configurations with different longitudinal slopes, expansion angles and cross slopes for fixed hydraulic conditions (Froude number, Strickler's roughness coefficient, etc.), presents several critical findings, as enumerated in the paragraphs below.

The reservoir geometry and bathymetry significantly influence the flow velocity which, in turn, dictates the conditions of sediment transport and deposition within the reservoir. The lateral spread of sediment increases with the increase of expansion angle resulting in lower peaks of sediment dunes. Increasing cross slope increases the velocity of flow, thereby causing significantly higher movement of sediments. Further, the cross slope also has a direct influence in increasing the inward (transverse) movement of sediment towards the central dip resulting in a narrower sediment footprint across the reservoir section.

The findings of this study contribute to the understanding of bed morphological processes in shallow trapezoidal reservoirs. However, secondary turbulent flow, which is often generated in a reservoir, has not been considered in the present depth-averaged model and therefore, the investigations of 3-D models are required.

ACKNOWLEDGEMENTS

The authors gratefully acknowledge the Department of Science and Technology, Government of India, for funding the research project. Thanks are also due to the Water Resources Department, Government of Odisha for providing the sedimentation reports of the Hirakud reservoir and to the Central Water Commission, Bhubaneswar, for providing relevant discharge and sediment data.

REFERENCES

Behrangi, F., Banihashemi, M. A., Mahani, Sh. & Rahmanian, M. R. (2014). Sediment settling in the Latian Dam in Iran. *International Journal of Sediment Research*, 29(2), 208-217.

Bluekenue, (2012). Visualization and analysis for hydraulic modelling, Version 3.3.25. Canadian Hydraulics Centre, National Research Council, Ottawa, Ontario, Canada.

Blumberg, A. F. & Mellor, G. L. (1987). A description of a three-dimensional coastal ocean circulation model. In Heaps, N.S., editor, Three-Dimensional Coastal Ocean Models, Coastal and Estuarin, American Geophys Union 1-16.

Camnasio, E., Orsi, E. & Schleiss, A. (2011). Experimental study of velocity fields in rectangular shallow reservoirs. *Journal of Hydraulic Research*, 49(3), 352–358.

Chang, H. H. (1998). Generalized computer program: Users' manual for FLUVIAL-12: Mathematical model for erodible channels, San Diego.

Desombre, J. (2013). TELEMAC Modelling System, Version 6.2, Operating Manual. EDF R&D (National Laboratory for Hydraulics and Environment) Chatou, France. Available on website www.openTELEMAC.org.

Dewals, B., Erpicum, S., Archambeau, P. & Pirotton, M. (2012). Experimental study of velocity fields in rectangular shallow reservoirs. *Journal of Hydraulic Research*, 50(4), 435-436.

DHI Inc. (2003). 301 South State Street, Newtown, PA, 18940, USA. http://www.dhisoftware.com

Dufresne, M., Dewals, B. J., Erpicum, S., Archambeau, P. & Pirotton, M. (2011). Numerical investigation of flow patterns in rectangular shallow reservoirs. *Engineering Applications of Computational Fluid Mechanics*, 5(2), 247-258.

Dutta, S. & Sen, D. (2016). Sediment Distribution and its Impact on Storage Capacity of Hirakud Reservoir. *Lakes and Reservoirs: Research and Management*, 21(3), 245–263.

Faghihirad, S., Lin, B. & Falconer, R. A. (2015). Application of a 3D layer integrated numerical model of flow and sediment transport processes to a reservoir. *Water*, 7 (10), 5239–5257.

Gao, P., Wang, Z. Y. & Siegel, D. (2015). Spatial and temporal changes of sedimentation in Three Gorges Reservoir of China. *Lakes and Reservoirs: Research and Management*, 20(4), 233-242.

Garde, R. J., Ranga Raju, K. G. & Sujudi, A. W. R. (1990). Design of settling basins. *Journal of Hydraulic Engineering*, 28(1), 81-91.

Hayter, E. J., Bergs, M. A., Gu, R., McCutcheon, S., Simth, S. J. & Whiteley, H. J. (1995). HSCTM-2D, A finite element model for depth averaged hydrodynamics, sediment and contaminant transport. National Exposure Research Laboratory, Office of Research and Development, UE Environmental Protection Agency, Athens, Georgia.

Hostache, R., Hissler, C., Matgen, P., Guignard, C. & Bates, P. (2014). Modelling suspended-sediment propagation and related heavy metal contamination in floodplains: a parameter sensitivity analysis. *Hydrological Earth System Sciences*, 18, 3539–3551.

HydroQual, (2002). A primer for ECOMSED, Users Manual, Version 1.3. HydroQual, Inc., Mahwah, NJ, USA, pp. 188.

Kantoush, S. A., De Cesare, G., Boillat, J. L. & Schleiss, A. J. (2008). Flow field investigation in a rectangular shallow reservoir using UVP, LSPIV and numerical modelling. *Flow Measurement and Instrumentation*, 19(34), 139-144.

Kantoush, S. A. & Schleiss, A. J. (2009). Channel formation during flushing of large shallow reservoirs with different geometries. *Environmental Technology*, 30(8), 855-863.

Lai, Y. G. (2008). SRH-2D Theory and User's Manual version 2.0, Technical Service Center, Bureau of Reclamation, Denver, CO.

Langendoen, E. J. (2000). CONCEPTS-Conservational channel evolution and pollutant transport system software manual. USDA-ARS Nationa Sedimentation Laboratory, Research Report 16, Oxford, Mississippi.

Lu, Y. J. & Wang, Z. Y. (2009). 3D numerical simulation for water flows and sediment deposition in dam areas of the Three Gorges Project. *Journal of Hydraulic Engineering*, 135(9), 755-769.

Mehta, A. J., Hayter, E. J., Parker, W. R., Krone, R. B. & Teeter, A. M. (1989). Cohesive sediment transport: Part I. Process description. *Journal of Hydraulic Engineering*, 115(8): 1076-1093.

Minh Duc, B., Wenka, T. & Rodi, W. (2004). Numerical modelling of bed deformation in laboratory channels. *Journal of Hydraulic Engineering*, 130(9), 894-904.

Morris, G. L. & Fan, J. (1998). Reservoir Sedimentation Handbook. Tata McGraw-Hill Publishing Company.

Olsen, N. R. B., Jimenez, O., Lovoll, A. & Abra-hamsen, L. (1994). Calculation of water and sediment flow in hydropower reservoirs. IAHR Int. Conf. on Modelling, Testing and Monitoring of Hydropower Plants, Budapest.

Papanicolaou, A. N. T., Elhakeem, M., Krallis, G., Prakash, S. & Edinger, J. (2008). Sediment transport modelling review-current and future developments. *Journal of Hydraulic Engineering*, 134(1): 1-14.

Peltier, Y., Erpicum, S., Archambeau, P., Pirotton, M. & Dewals, B. (2014). Experimental investigation of meandering jets in shallow reservoirs. *Environmental Fluid Mechanics*, 14(3), 699-710.

Rahmanian, R. & Banihashemi, A. (2011). Sediment distribution pattern in some Iranian dams based on a new empirical reservoir shape function. *Lake and Reservoir Management*, 27(3), 245-255.

Ranga Raju, K. G., Kothyari, U. C., Srivastav, S. & Saxena, M. (1999). Sediment removal efficiency of settling basins. *Journal of Irrigation and Drainage Engineering*, 125(5), 308-314.

Stone, M., Chen, L. & Scott, S. (2007). Guidance for modelling of sedimentation in stream restoration projects. Desert Research Institute, Nevada System of Higher Education. Prepared for U.S. Army Corps of Engineers, Engineer Research and Development Center.

Stovin, V. R. (1996). The prediction of sediment deposition in storage chambers based on laboratory observations and numerical simulation. PhD Thesis, Department of Civil and Structural Engineering, University of Sheffield, Sheffield.

Tassi, P. (2014). Sisyphe Version 6.3, User's Manual. EDF R&D (National Laboratory for Hydraulics and Environment) Chatou, France. Available on website www.openTELEMAC.org.

Thomas, W. A. & McAnally, W. H. (1990). User's Manual for the Generalized Computer Program Systems for Open Channel Flow and Sedimentation: TABS-2 system, US Army Corps of Engineers, Waterways Experiment Station, Hydraulics Laboratory, Vicksburg, MS.

USACE, (1993). River Hydraulics, EM 1110-2-1416, U. S. Army Corps of Engineers, October 1993.

Villaret, C., Hervouet, J. M., Kopmann, R., Merkel, U. & Davies, A. G. (2013). Morphodynamic modeling using the Telemac finite element system, *Computers and Geosciences*, 53, 105–113.

White, W. R. (2001). Evacuation of sediments from reservoirs, Thomas Telford Publishing, London.

WL | Delft Hydraulics, (2006). Dune erosion, large scale model tests and dune erosion prediction method. WL |Delft Hydraulics report H4357, January 2006.

Wu, W. (2001). CCHE2D-2.1, Sediment Transport model, Technical report no. NCCHE-TR-2001-3, National Center for Computational Hydroscience and Engineering, The University of Mississippi.

Wu, W. & Vieira, D. A. (2002). One-dimensional channel network model CCHE1D Version 3.0 − Technical Manual. Technical Report No. NCCHE-TR-2002-1, National Center for Computational Hydroscience and Engineering, The University of Mississippi.

Wu, W. & Wang, SSY. (2004). Depth averaged 2-D calculation of flow and sediment transport in curved channels. *International Journal of Sediment Research*, 19(4), 241-257.

Zhou, G., Wang, H., Shao, X. J. & Jia, D. D. (2009). Numerical model for sediment transport and bed degradation in the Yangtze River channel downstream of Three Gorges Reservoir. *Journal of Hydraulic Engineering*, 135(9), 729-740.

Data Availability Statement

Data derived from public domain resources: http://indiawris.gov.in/wris/#/riverPoint

Hosted file

`paper.doc` available at https://authorea.com/users/284695/articles/407613-numerical-simulations-to-understand-spatial-sedimentation-characteristics-in-a-shallow-reservoir

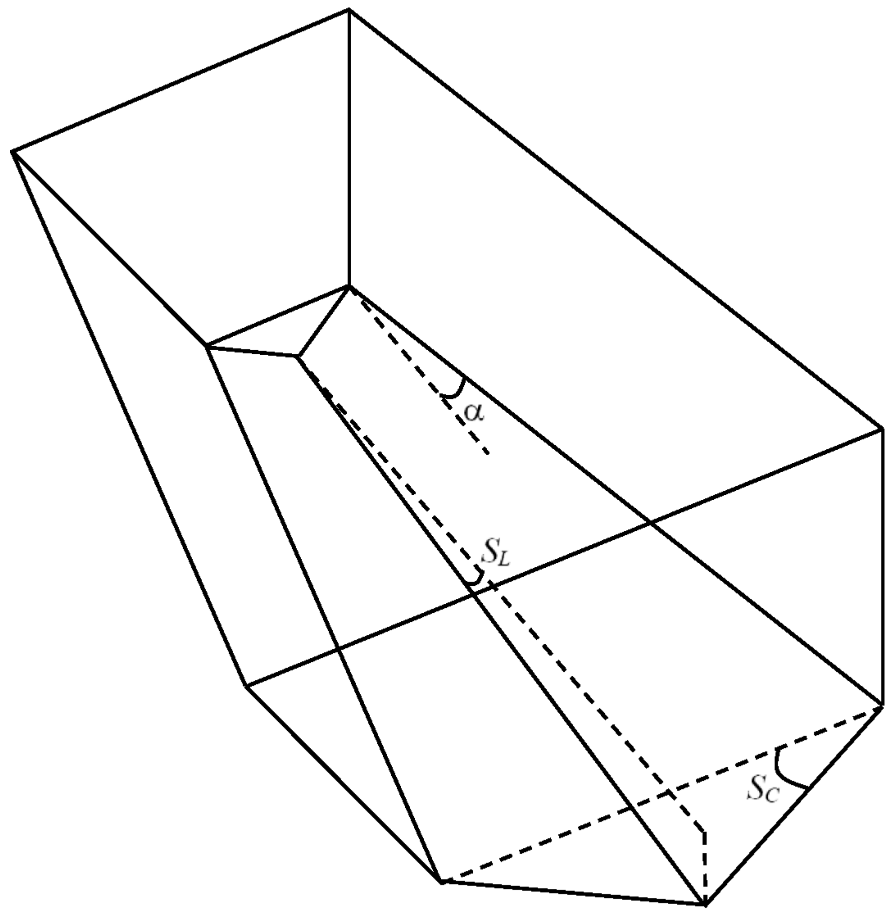

Figure 1 Schematic of modelled reservoir geometry

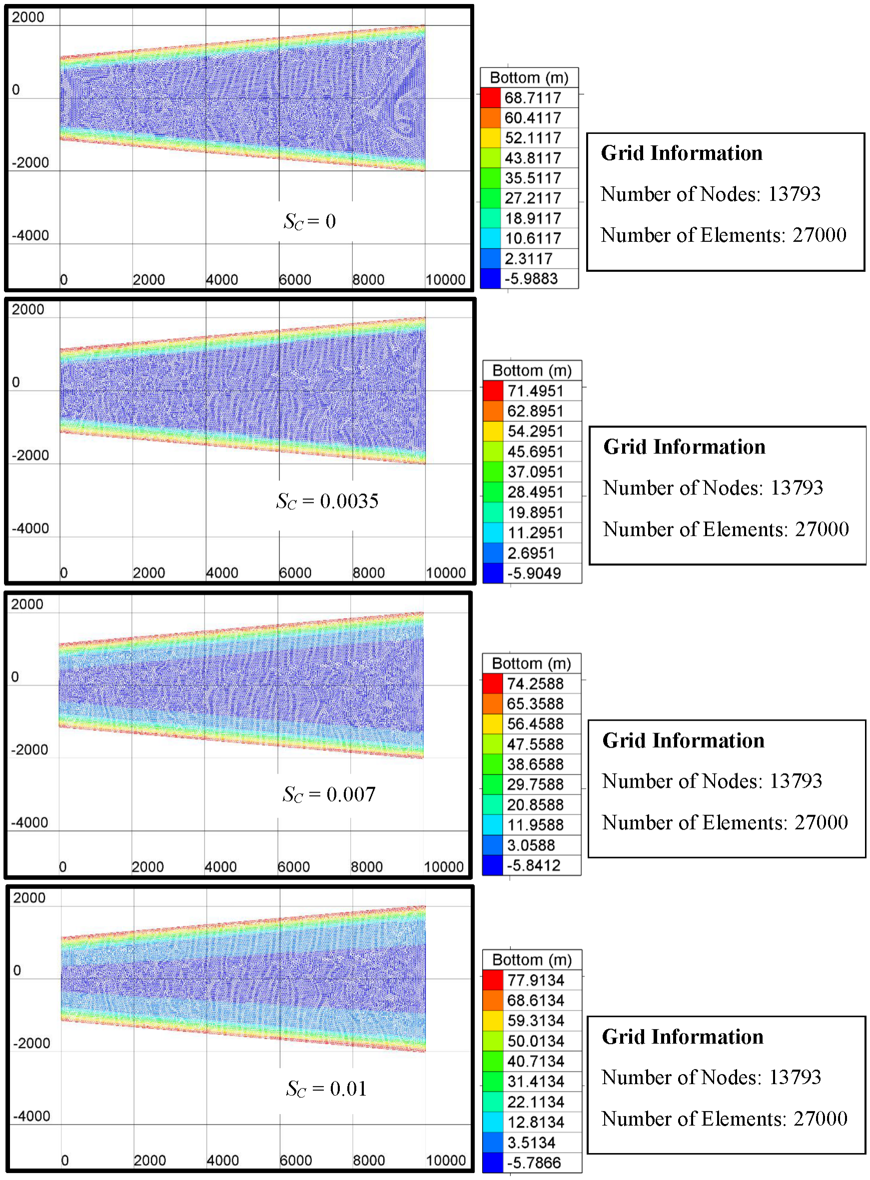

Figure 2(a) Computational mesh of trapezoidal reservoirs for various cross slopes, fixed longitudinal slope (0.0006) and expansion angle (5°)

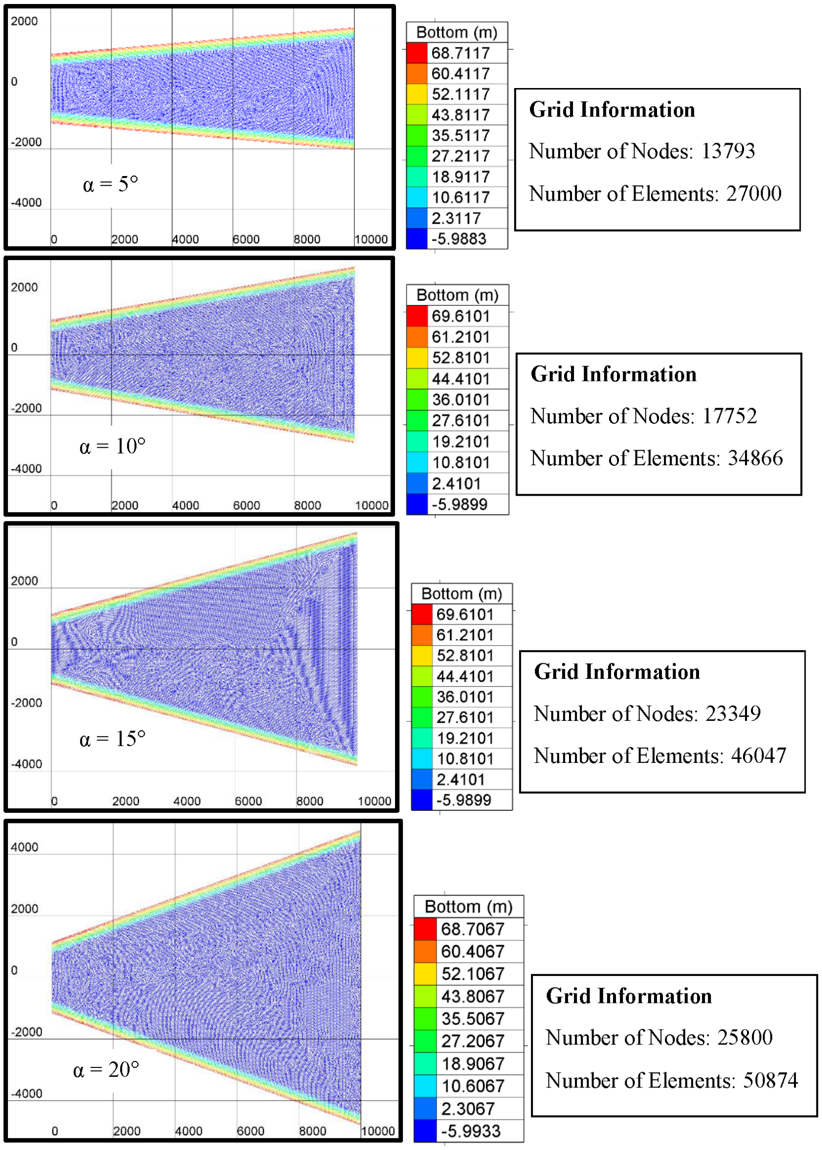

Figure 2(b) Computational mesh of flat trapezoidal reservoirs for various expansion angles and fixed longitudinal slope (0.0006)

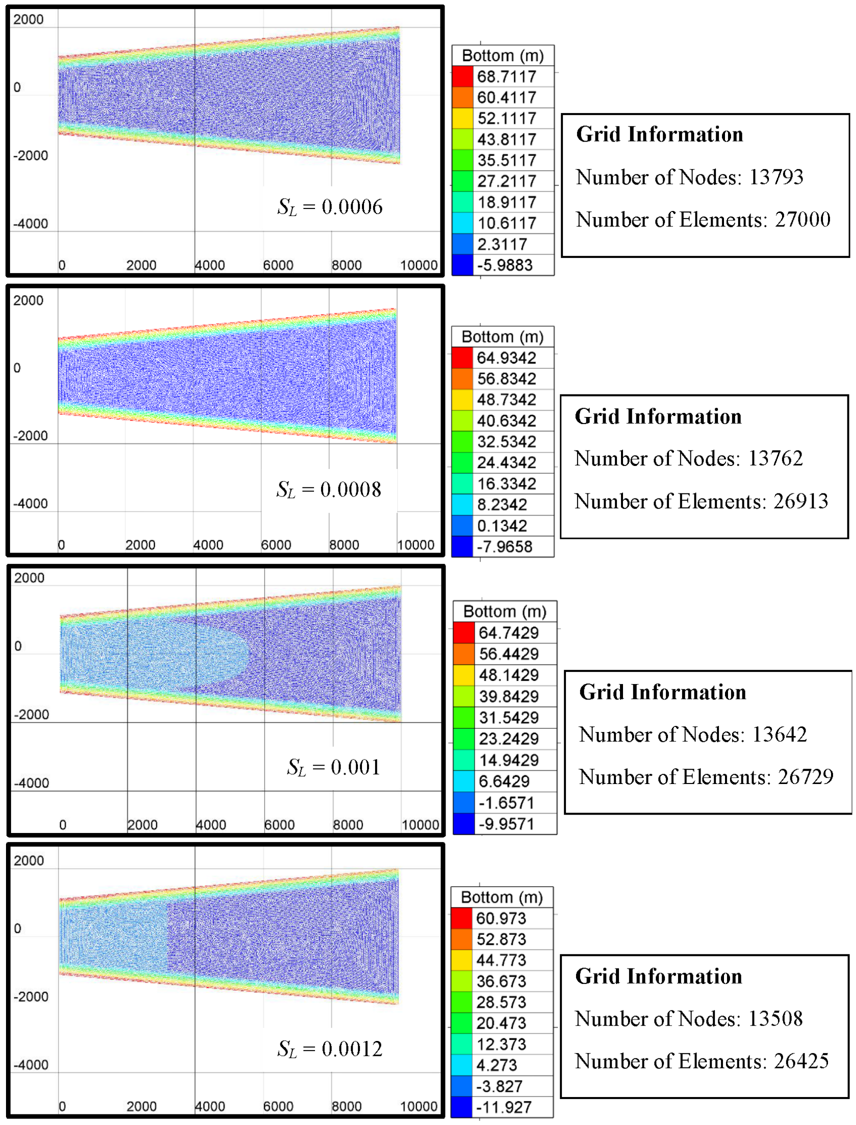

Figure 2(c) Computational mesh of flat trapezoidal reservoirs for various longitudinal slopes and fixed expansion angle (5°)

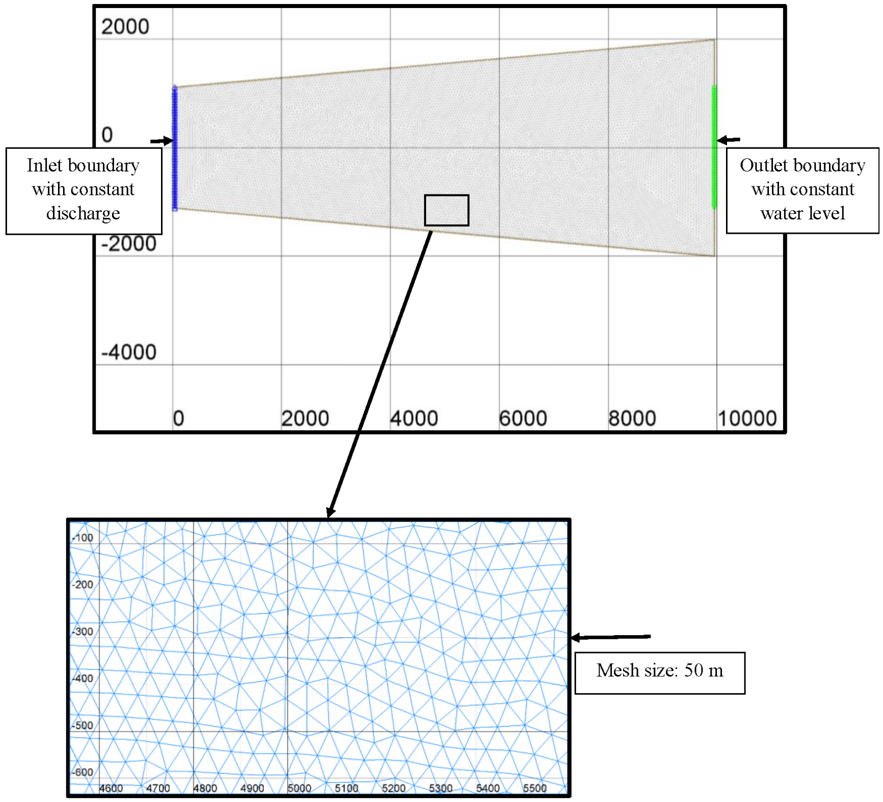

Figure 3 Boundary definitions in the computational domain

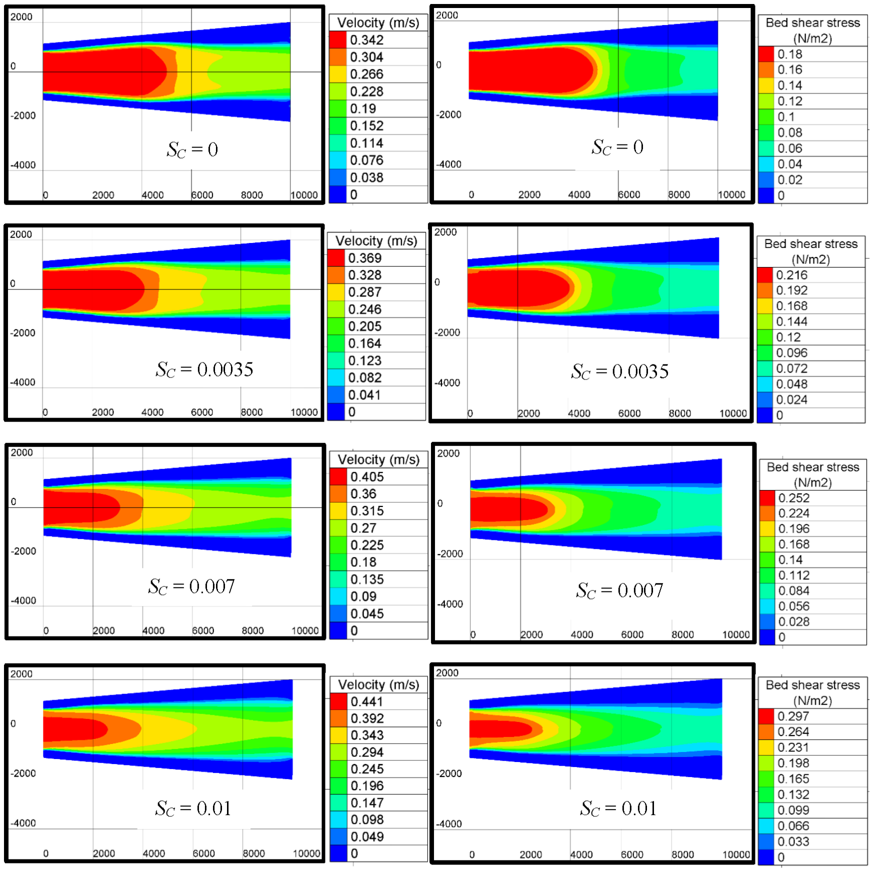

Figure 4(a) Contours of velocity and bed shear stress of trapezoidal reservoirs for various cross slopes, fixed longitudinal slope (0.0006) and expansion angle (5°)

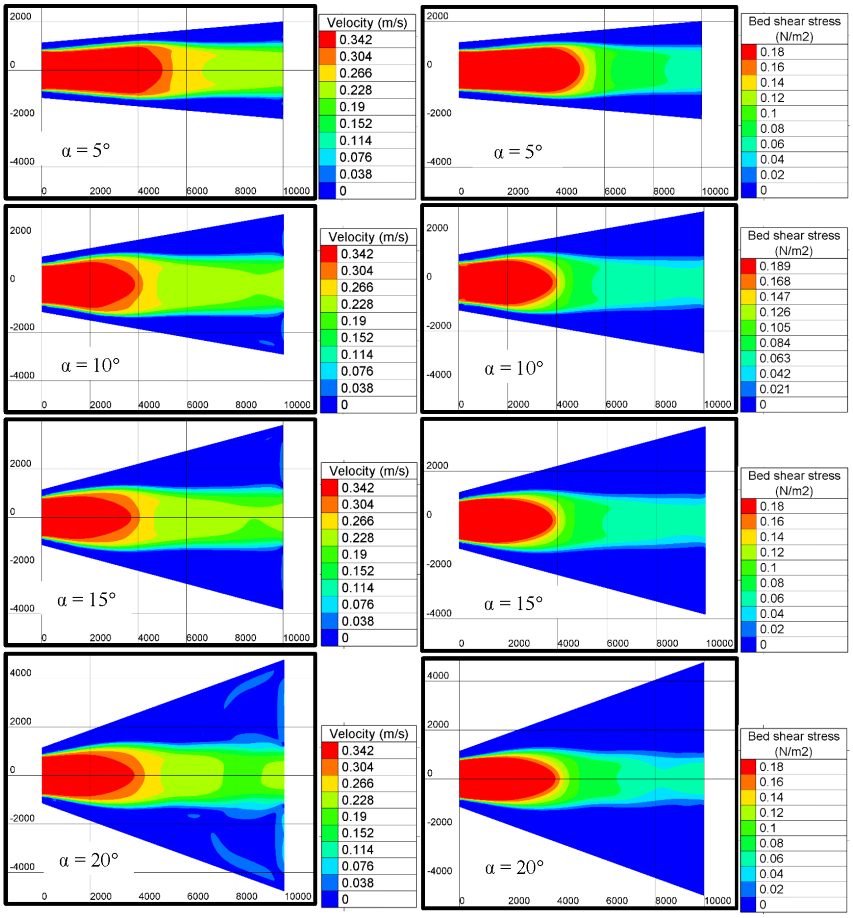

Figure 4(b) Contours of velocity and bed shear stress of flat trapezoidal reservoirs for various expansion angles and fixed longitudinal slope (0.0006)

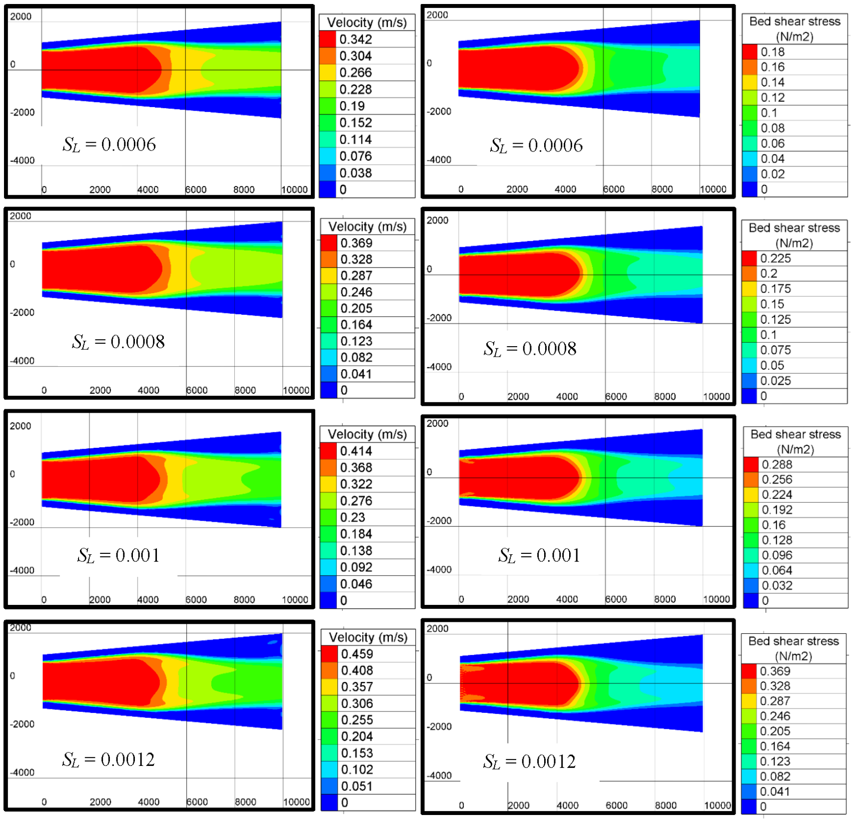

Figure 4(c) Contours of velocity and bed shear stress of flat trapezoidal reservoirs for various longitudinal slopes and fixed expansion angle (5°)

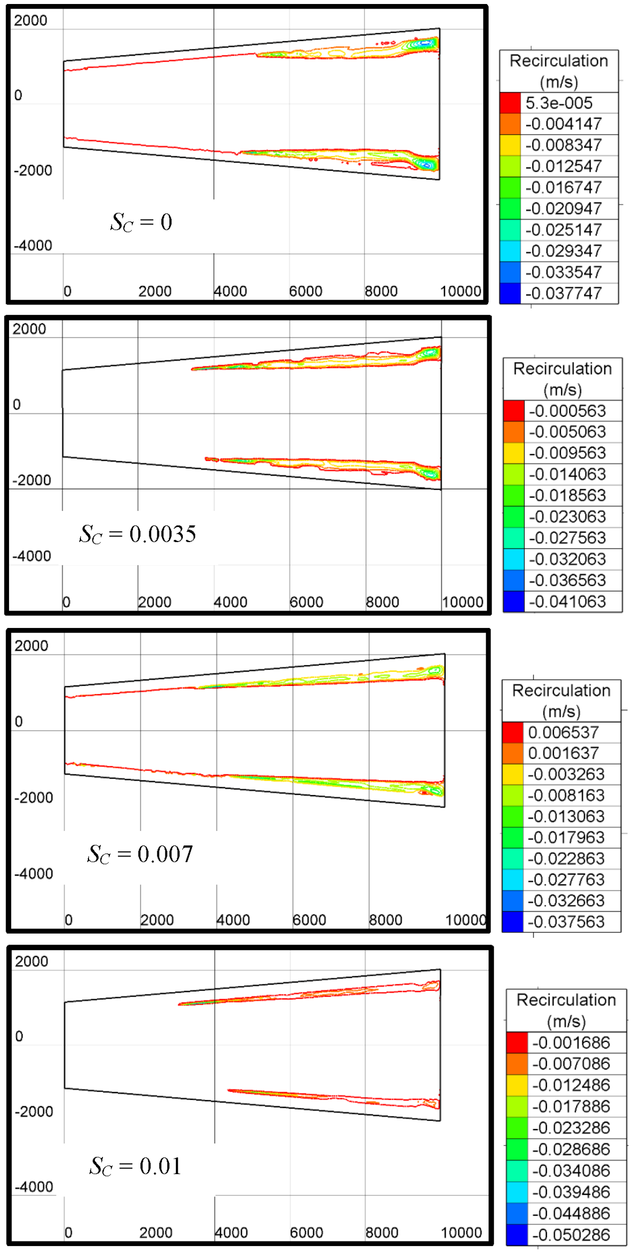

Figure 5(a) Recirculation of trapezoidal reservoirs for various cross slopes, fixed longitudinal slope (0.0006) and expansion angle (5°)

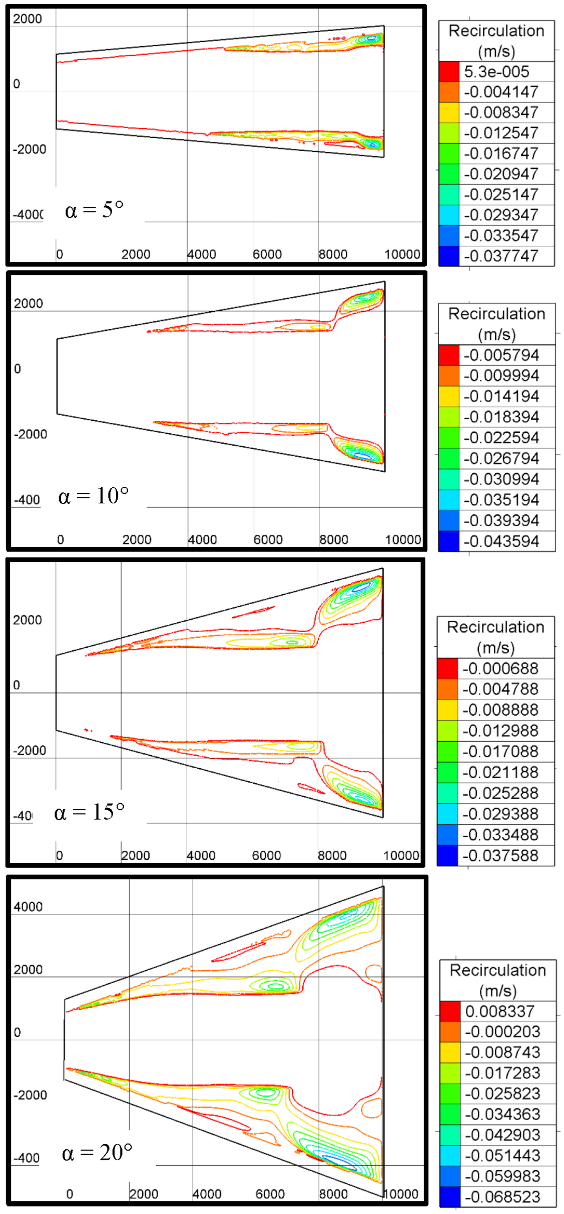

Figure 5(b) Recirculation of flat trapezoidal reservoirs for various expansion angles and fixed longitudinal slope (0.0006)

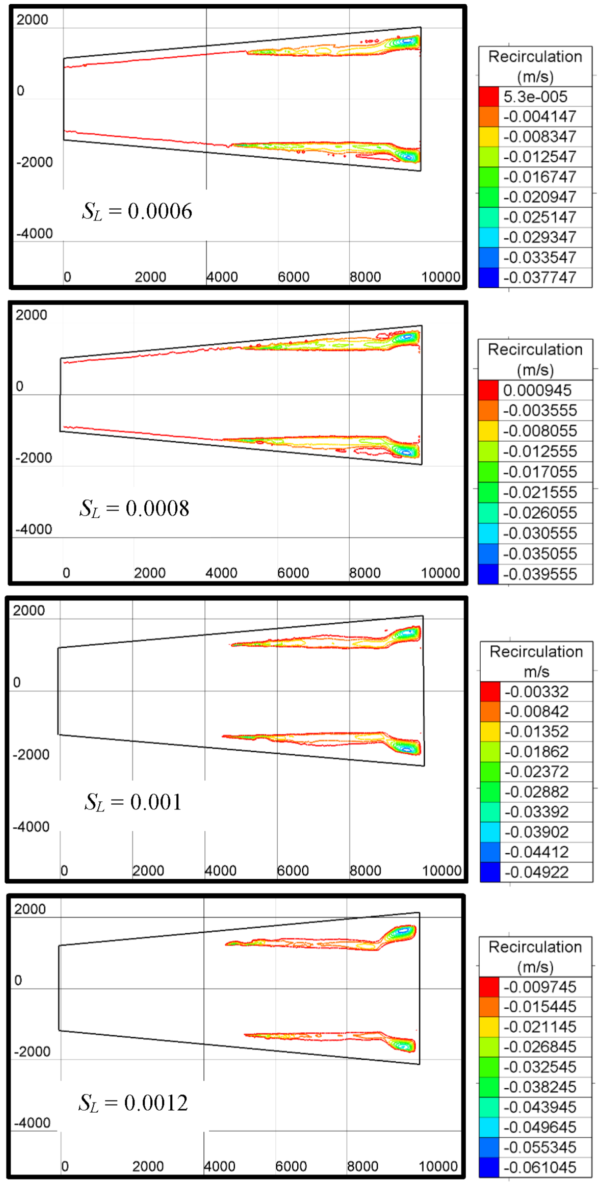

Figure 5(c) Recirculation of flat trapezoidal reservoirs for various longitudinal slopes and fixed expansion angle (5°)

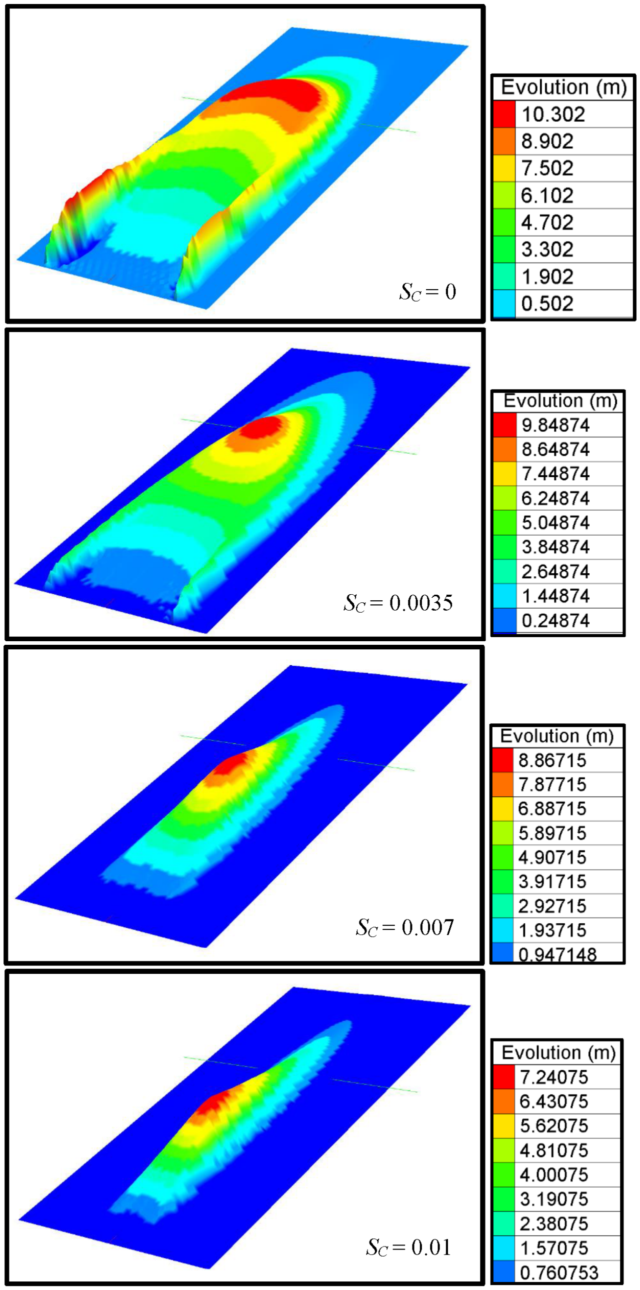

Figure 6(a) Morphological changes of trapezoidal reservoirs for various cross slopes, fixed longitudinal slope (0.0006) and expansion angle (5°)

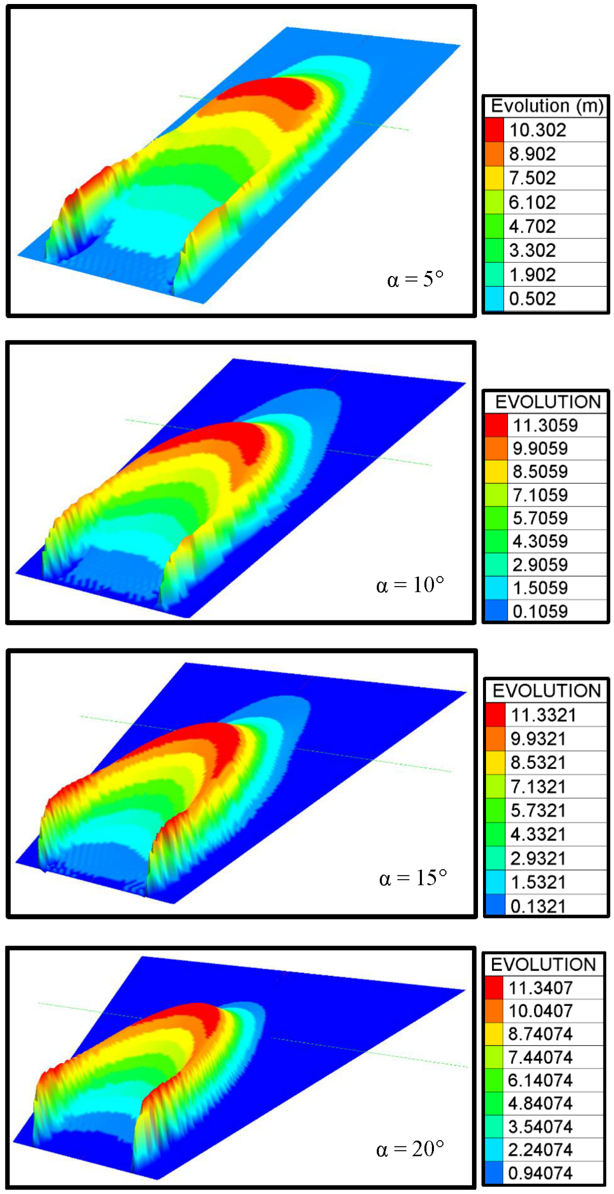

Figure 6(b) Morphological changes of flat trapezoidal reservoirs for various expansion angles and fixed longitudinal slope (0.0006)

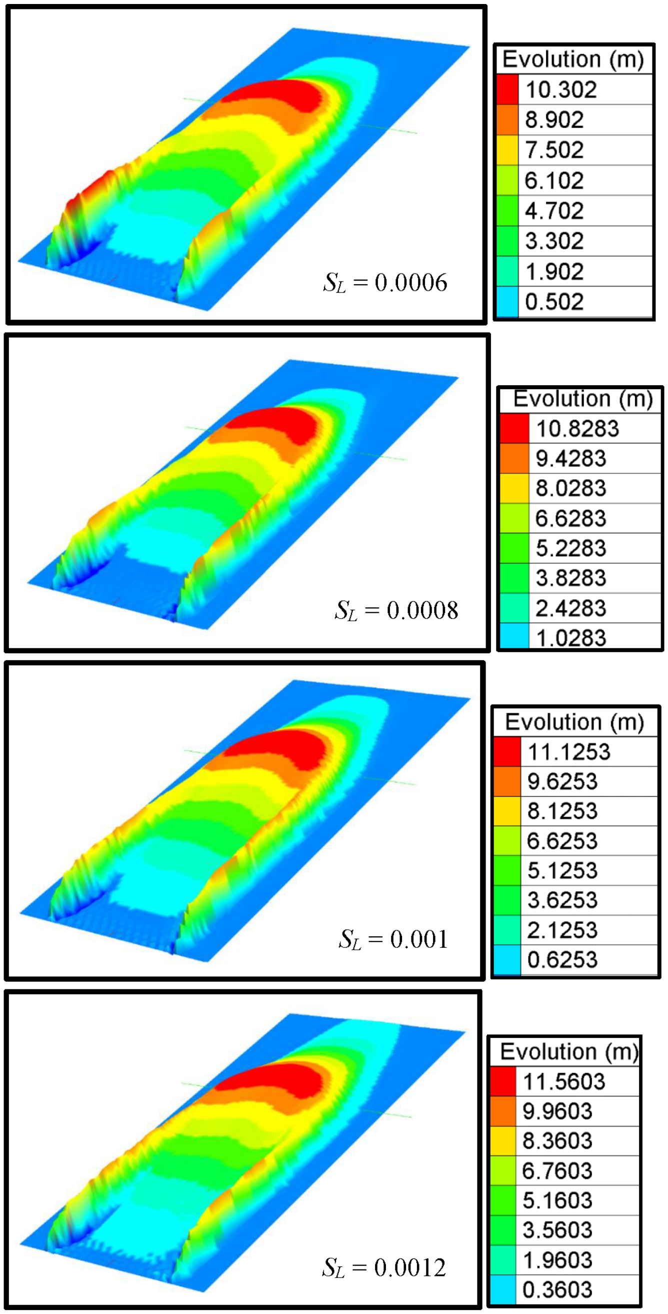

Figure 6(c) Morphological changes of flat trapezoidal reservoirs for various longitudinal slopes and fixed expansion angle (5°)

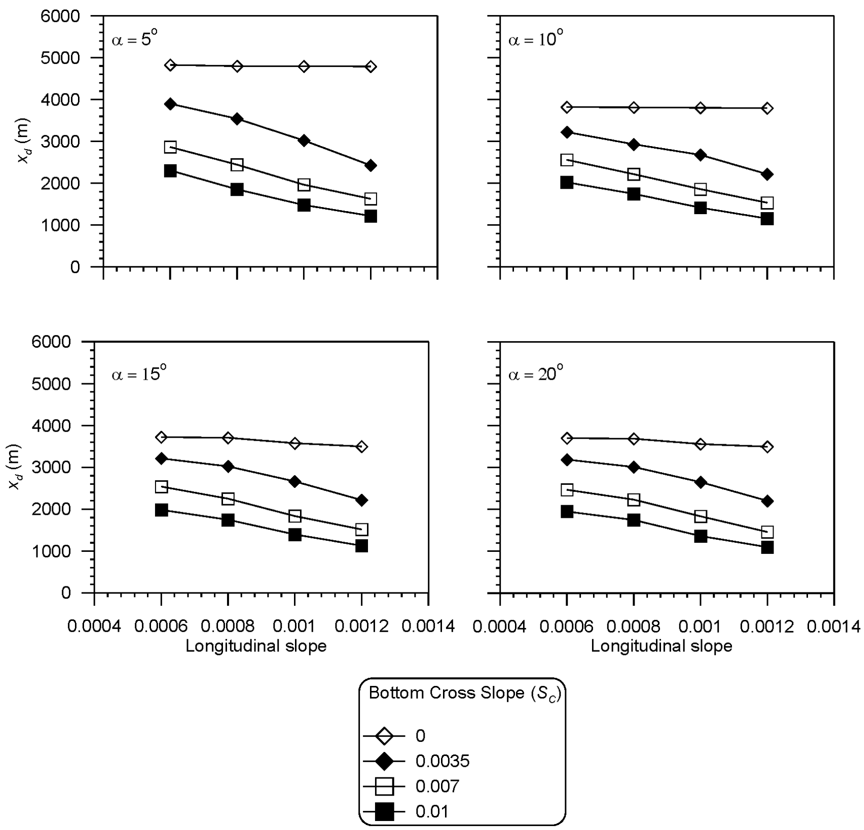

Figure 7 Variations of longitudinal distances (x_d) at which the maximum evolution occurs versus longitudinal slope

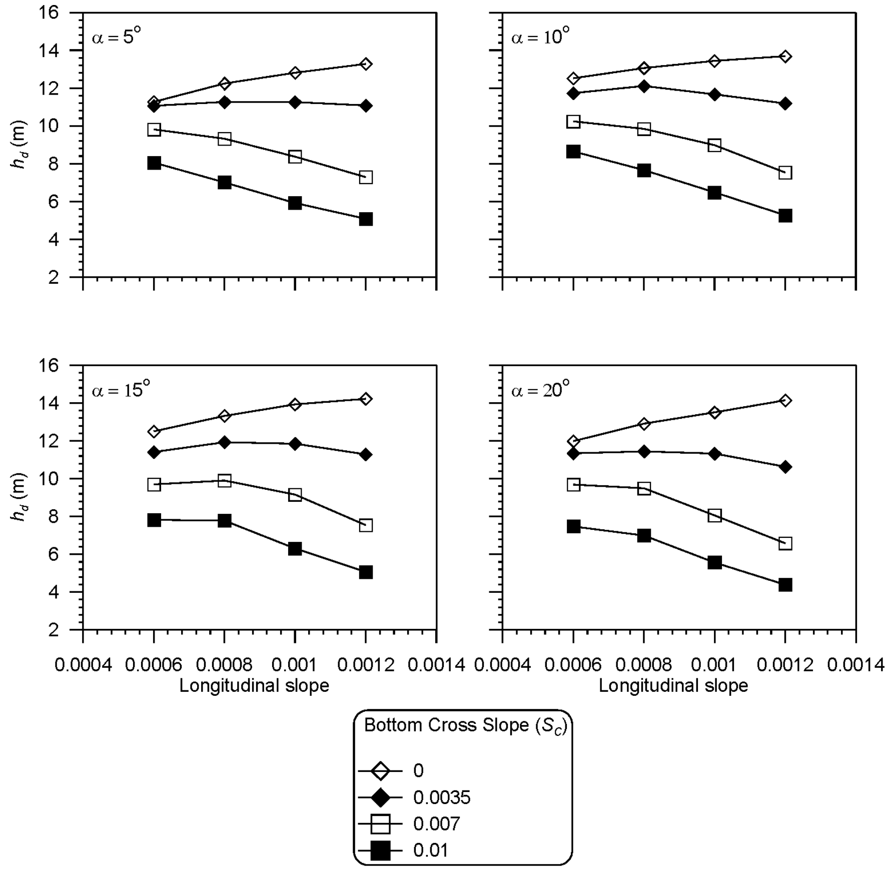

Figure 8 Maximum height of evolutions (h_d) versus longitudinal slope

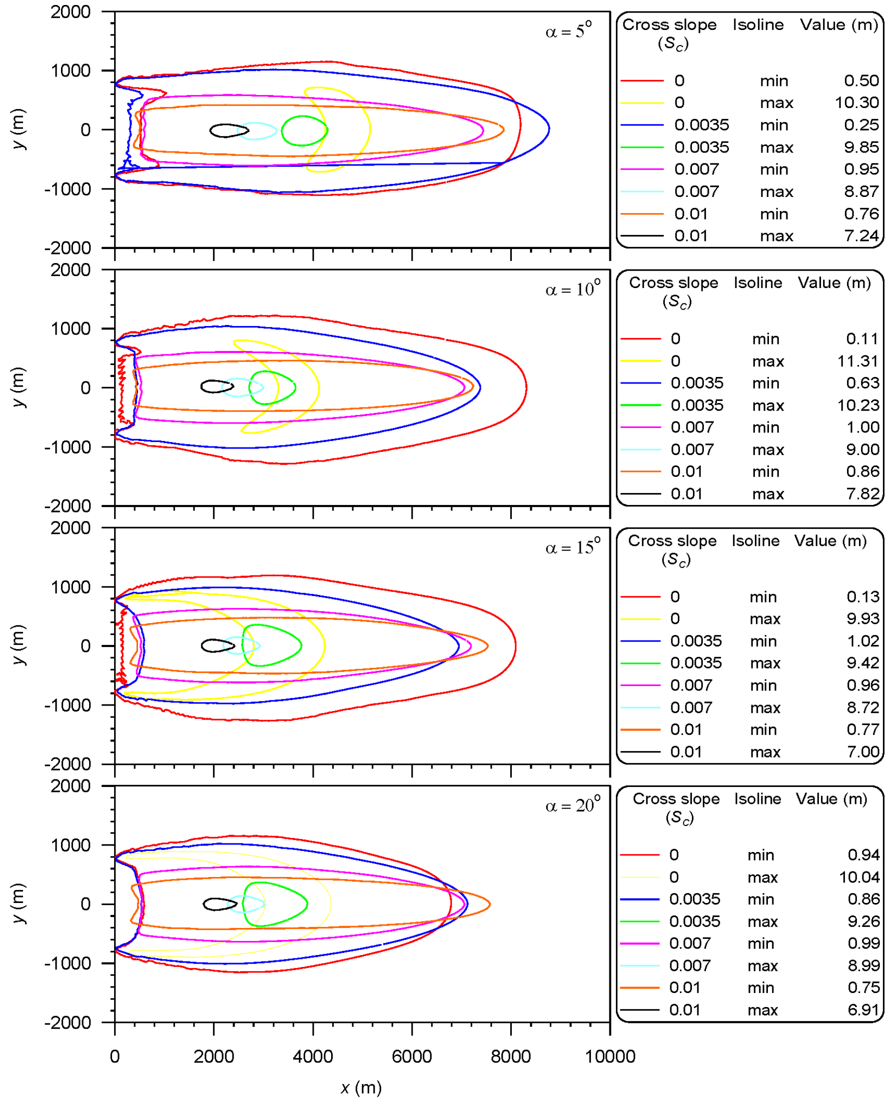

Figure 9(a) Minimum and maximum isolines for constant $S_L = 0.0006$

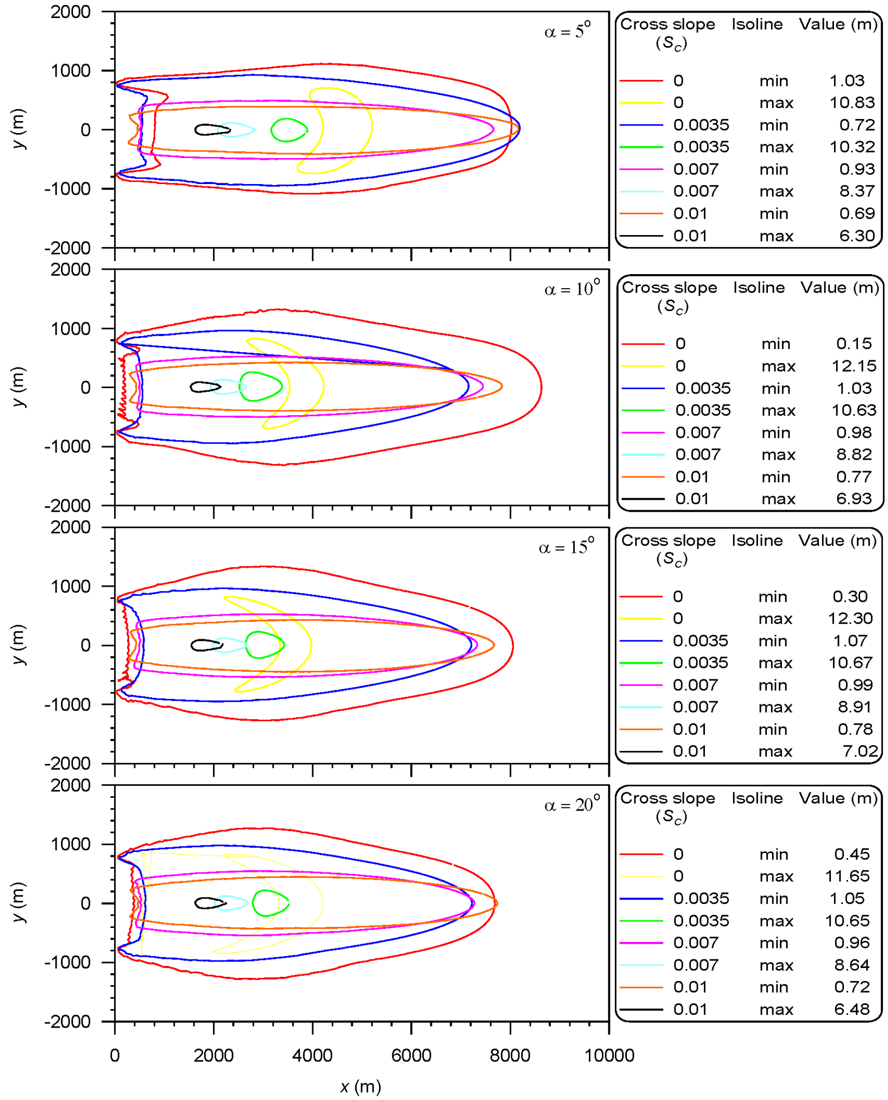

Figure 9(b) Minimum and maximum isolines for constant $S_L = 0.0008$

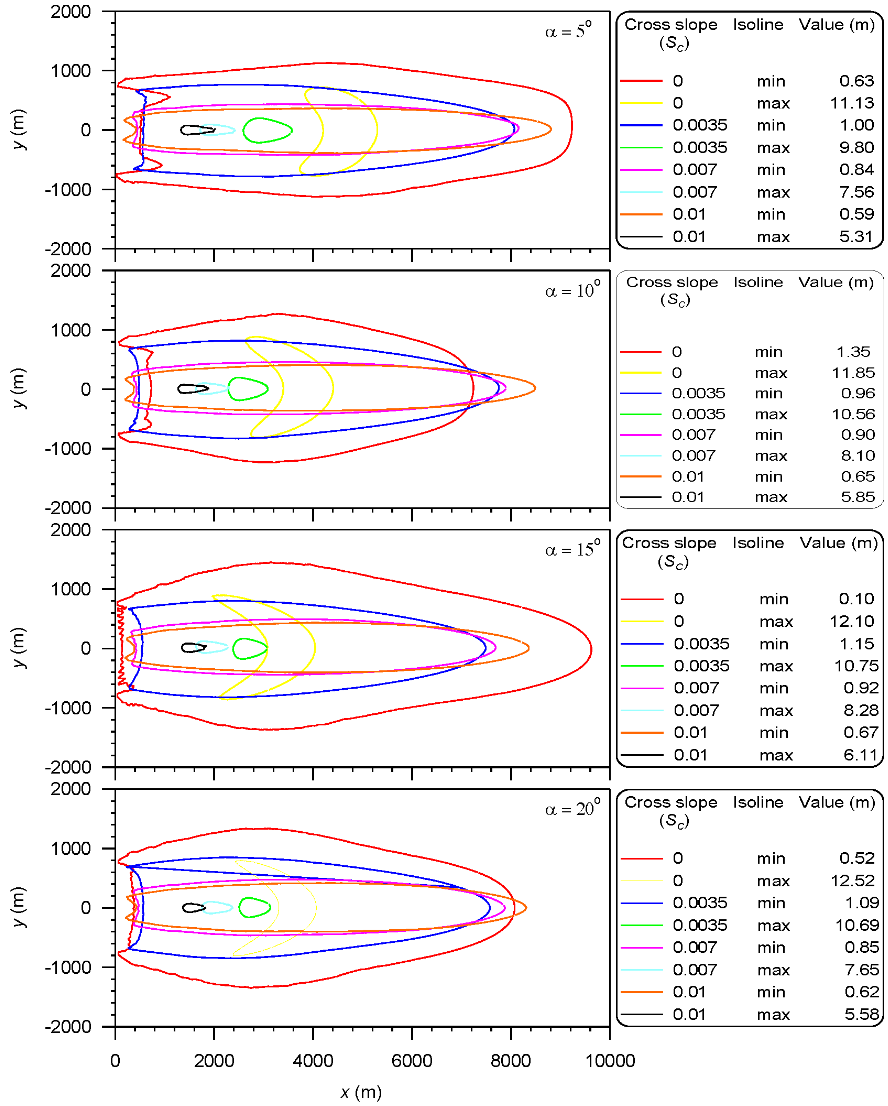

Figure 9(c) Minimum and maximum isolines for constant $S_L = 0.001$

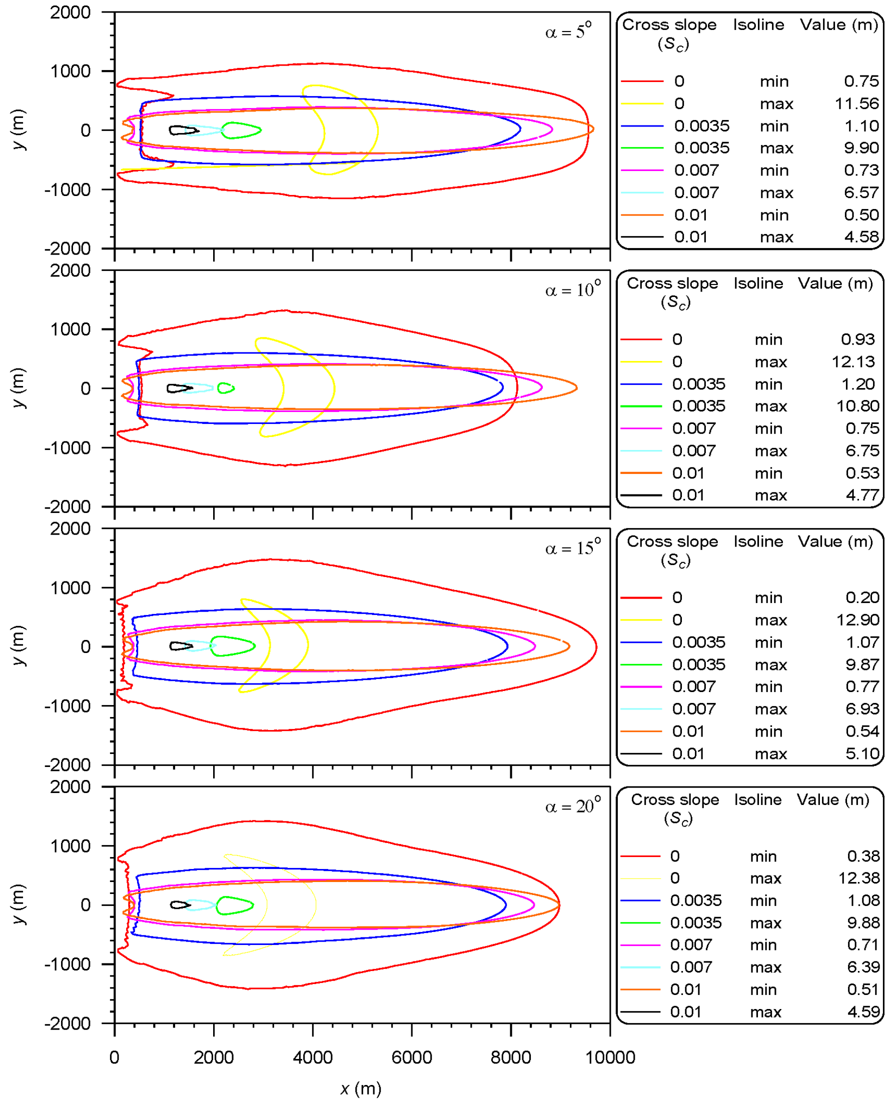

Figure 9(d) Minimum and maximum isolines for constant $S_L = 0.0012$

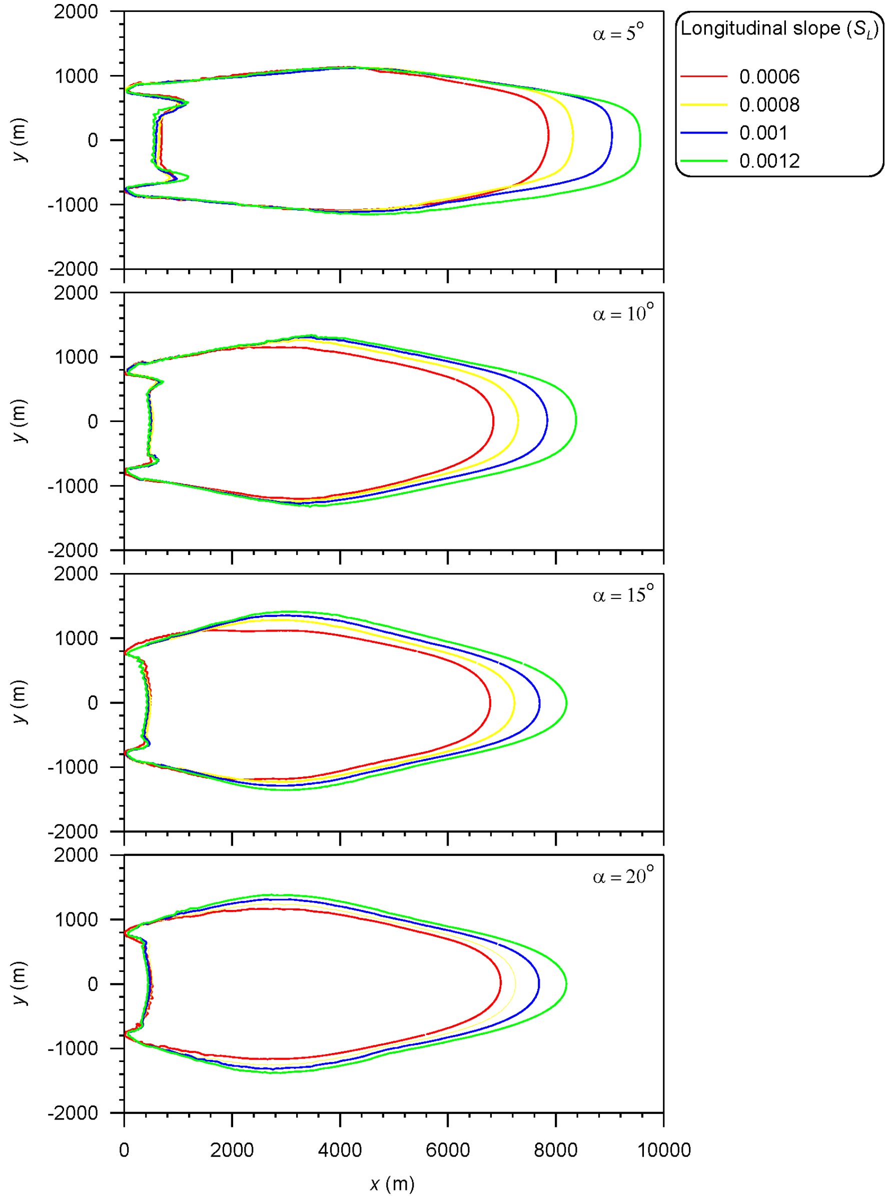

Figure 10 Isolines of 0.75 m for flat bottom reservoir

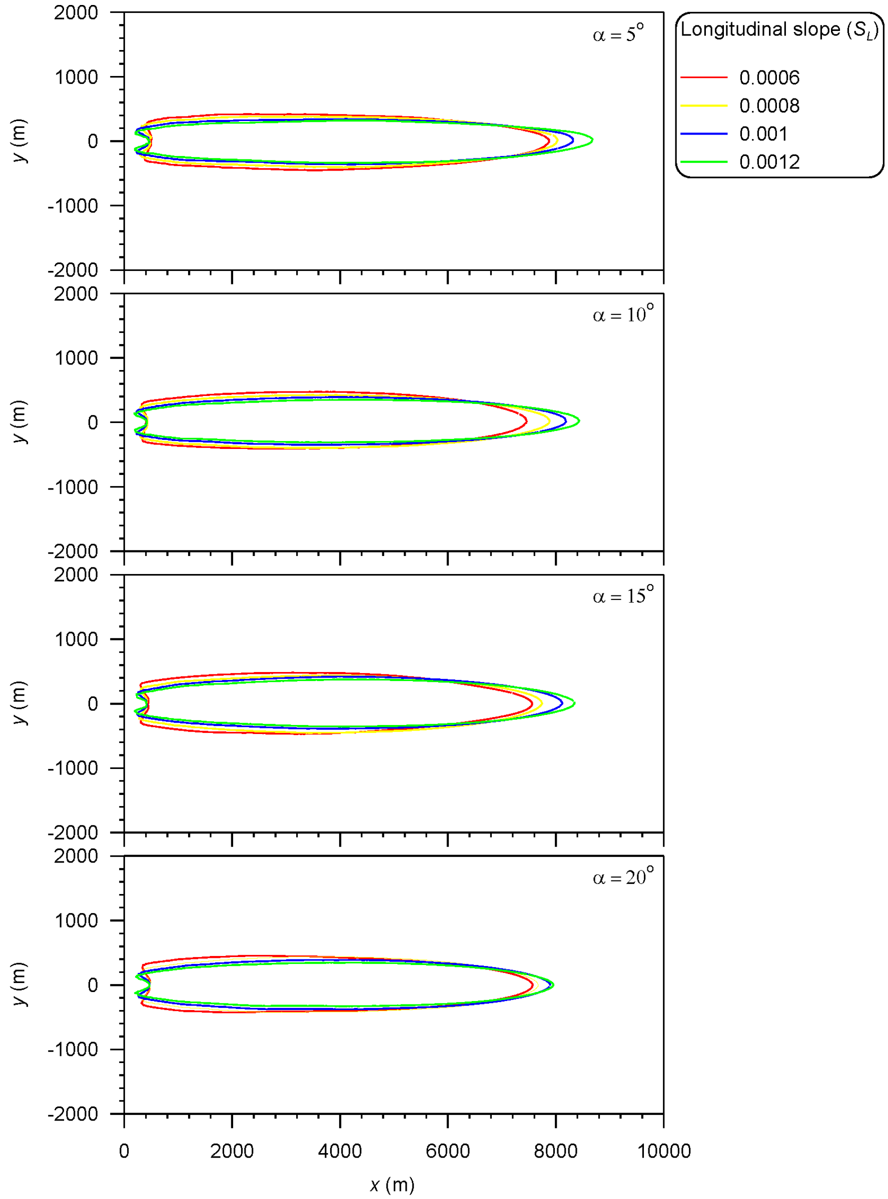

Figure 11 Isolines of 0.75 m for V-shaped reservoir (S_C = 0.01)

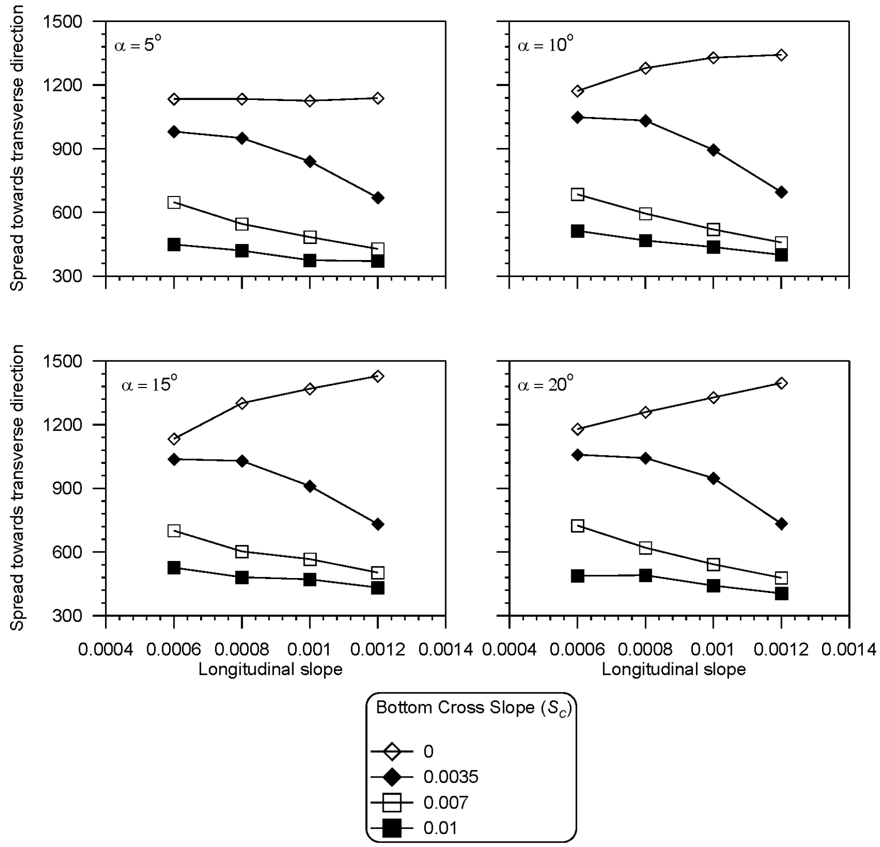

Figure 12 Variation of sediment distribution in the transverse direction versus longitudinal slope

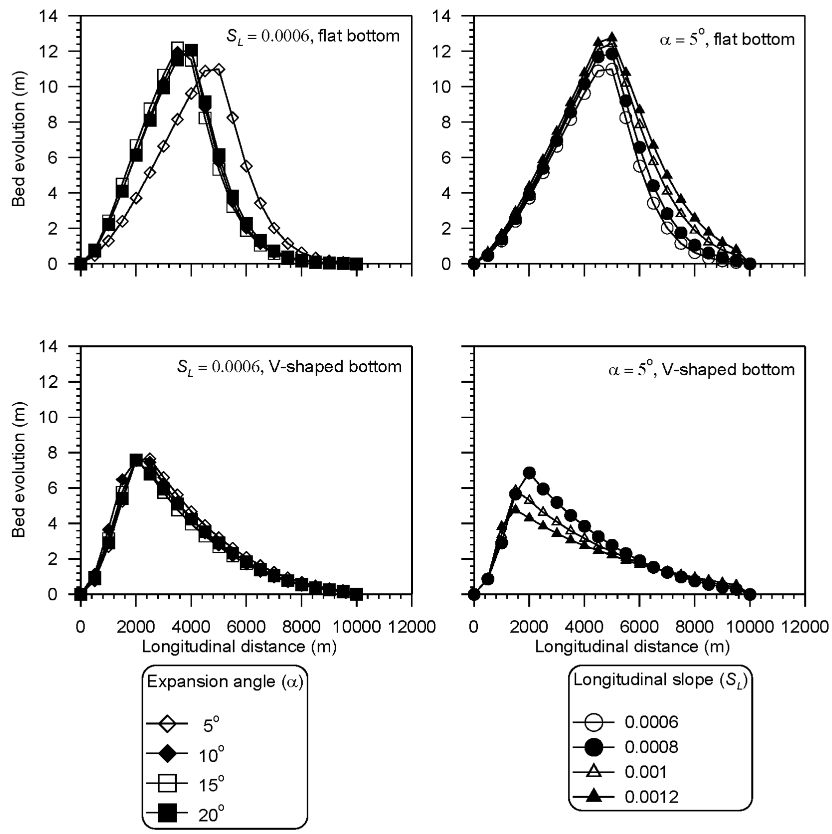

Figure 13 Variation of bed evolution versus longitudinal distance for flat and V-shaped reservoirs

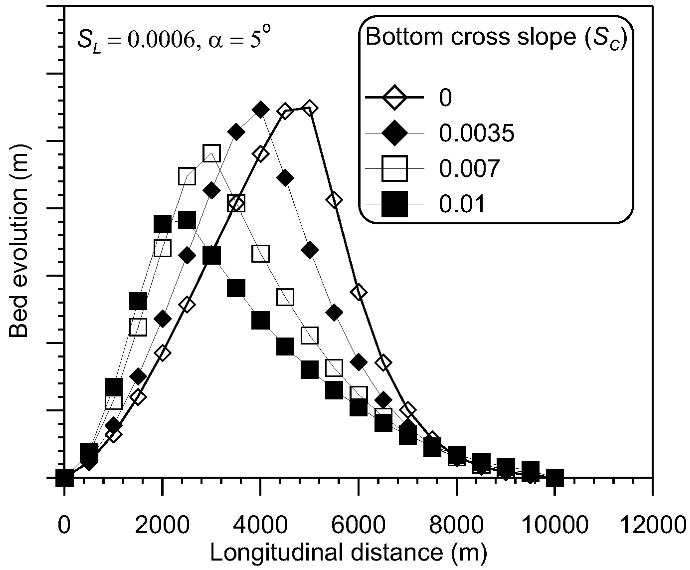

Figure 14 Variation of bed evolution versus longitudinal distance for fixed longitudinal slope and expansion angle

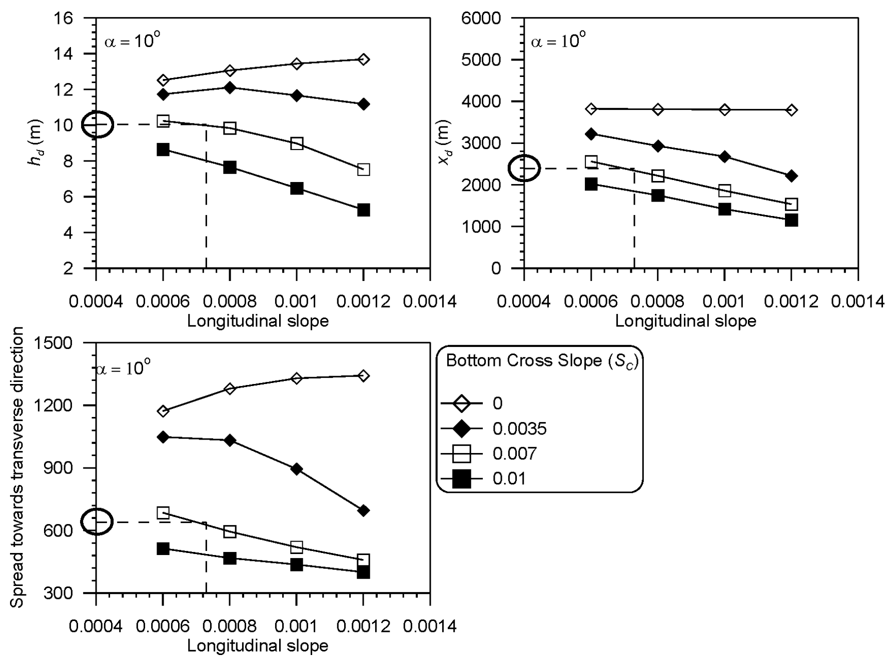

Figure 15 Variation of sediment distribution versus longitudinal slope

*Note: Dotted line represents the parameters for the Mahanadi River

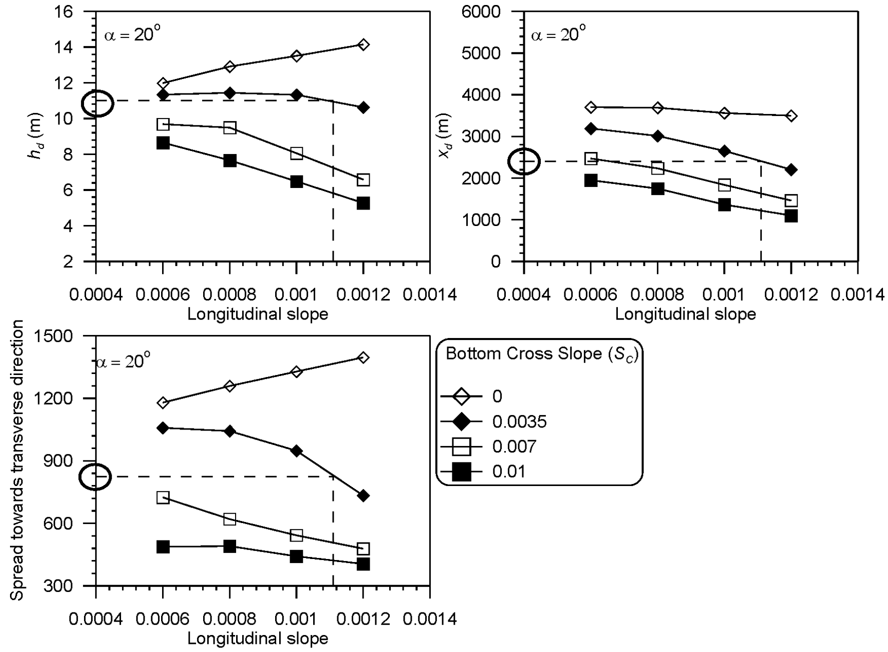

Figure 16 Variation of sediment distribution versus longitudinal slope

*Note: Dotted line represents the parameters for the Ib River

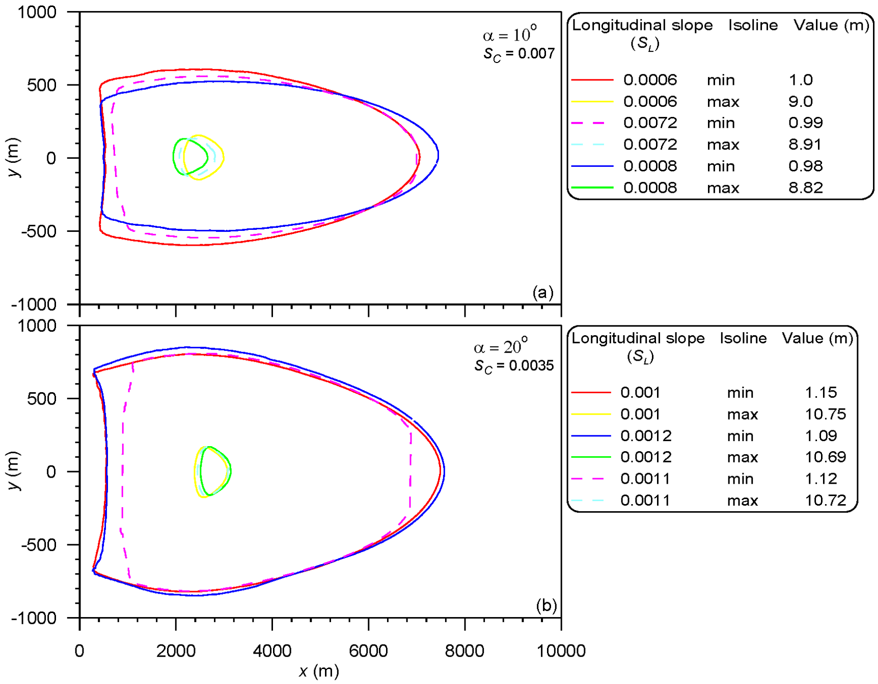

Figure 17 Minimum and maximum isolines for various expansion angles, longitudinal and cross slopes

*Note: Dotted line represents the Isolines for the (a) Mahanadi and (b) Ib Rivers

Hosted file

`Table 1.docx` available at https://authorea.com/users/284695/articles/407613-numerical-simulations-to-understand-spatial-sedimentation-characteristics-in-a-shallow-reservoir

Hosted file

`Table 2.docx` available at https://authorea.com/users/284695/articles/407613-numerical-simulations-to-understand-spatial-sedimentation-characteristics-in-a-shallow-reservoir